Am J Cancer Res 2022;12(9):4343-4360
www.ajcr.us /ISSN:2156-6976/ajcr0143901

Original Article

TOP2A inhibition reverses drug resistance of hepatocellular carcinoma to regorafenib

Zongwen Wang[1], Qiankun Zhu[1], Xiaodong Li[1], Xiaohang Ren[1], Jingtao Li[1], Yao Zhang[1], Shicong Zeng[1], Lishan Xu[1], Xiaoqun Dong[2], Bo Zhai[1]

[1]*Department of Surgical Oncology and Hepatobiliary Surgery, The Fourth Affiliated Hospital of Harbin Medical University, Harbin 150001, Heilongjiang, China;* [2]*The Liver Research Center of Rhode Island Hospital/Lifespan; Department of Medicine, The Warren Alpert Medical School of Brown University, Providence, RI 02903, USA*

Received May 4, 2022; Accepted September 12, 2022; Epub September 15, 2022; Published September 30, 2022

Abstract: Hepatocellular carcinoma (HCC) is the third leading cause of cancer-related death attributed to high frequency of metastasis and multiple drug resistance. We aim to examine the underlying molecular mechanism and to seek potential strategies to reverse primary/acquired resistance to regorafenib. Topoisomerase IIα (TOP2A) is critical for tumorigenesis and carcinogenesis. Clinically, high-TOP2A expression was correlated to shorter overall survival (OS) of patients, but its role in drug resistance of HCC remains unknown. Here, we screened the expression profiling of TOP2A in HCC and identified TOP2A as an upregulated gene involved in the resistance to regorafenib. Sustained exposure of HCC cells to regorafenib could upregulate the expression of TOP2A. Silencing TOP2A enhanced HCC cells' sensitivity to regorafenib. TOP2A inhibition by doxorubicin or epirubicin synergized with regorafenib to suppress the growth of sorafenib-resistant HCC tumors that possessed the sorafenib-resistant features both *in vitro* and *in vivo*. Thus, targeting TOP2A may be a promising therapeutic strategy to alleviate resistance to regorafenib and thus improving the efficacy of HCC treatment.

Keywords: TOP2A, regorafenib, hepatocellular carcinoma

Introduction

Liver cancer ranks the third leading cause of cancer-related deaths worldwide, with an estimated 906,000 new cases and 830,000 deaths in 2020 [1, 2], Liver cancer exhibits an extremely high degree of malignancy, developmental concealment, and rapid progression. Thus, it is asymptomatic in its early stage, causing delays in timely diagnosis [1, 3, 4]. Hepatocellular carcinoma (HCC) accounts for ~90% of primary liver cancer burden [1, 3]. For early-stage HCC, surgical resection, radiofrequency ablation, liver transplantation, or transarterial embolization (TACE) can extend patients' life expectancy [3]. However, over 80% of patients with HCC are diagnosed at an advanced stage disease and therefore cannot be treated with available therapeutic options [1, 3, 5]. Patients diagnosed with advanced stage HCC are ineligible for curative surgery, so therapeutic options are very limited in availability and efficacy. Currently, treatment for advanced-stage HCC is limited to systemic therapy [1, 3, 5].

Regorafenib, a multi-kinase inhibitor targeting the RAS/RAF/MEK/ERK pathway, has been approved to treat advanced/metastatic HCC as a second-line systemic therapy by the US Food and Drug Administration (USFDA) in April 2017 [6]. Similar with the first-line systemic drug sorafenib, regorafenib is an oral tyrosine kinase inhibitor that targets vascular endothelial growth factor receptors (VEGFRs), platelet-derived growth factor receptor beta (PDGFR-β), fibroblast growth factor receptor 1 (FGFR1), receptor tyrosine kinases (RET), Raf, angiopoietin-1 receptor (TIE-2), as well as kinases KIT and B-RAF [7-9]. However, regorafenib prolonged overall survival (OS) of patients who had disease progression after failure with sorafenib by only 2.8 months. Its efficacy was significantly reduced by primary or acquired resistance [10].

To date, few studies have investigated molecular mechanisms underlying resistance to regorafenib in human HCC.

DNA topoisomerases II are enzymes essential for DNA replication, transcription, and recombination, as well as for chromosome compaction and segregation. In eukaryotes, topoisomerases present as homodimers, and each subunit is composed of three functional domains (signal transduction region, ATPase domain and broken heavy chain region) [11]. The signal transduction region at the C-terminal is mainly related to DNA recognition, and the rest are the main active regions. The enzyme binds to DNA substrate with abnormal conformation through non-covalent bonds to form a complex. After introducing negative supercoil, the nick is connected. The whole process is as follows: (1) double stranded carbon skeleton of DNA is broken, making it easy to pass through the gap and change topological state; (2) ATP hydrolysis enables topoisomerase to undergo configuration conversion and be returned to normal structure [12, 13]. There are two isoforms of topoisomerase II in humans, α (TOP2A) and β (TOP2B), located on chromosomes 17q21-22 and 3p24, respectively. TOP2A is essential for survival and growth [12-14]. During DNA transcription, TOP2A removes DNA supercoiling. At the end of DNA replication, TOP2A is essential for chromosome condensation and segregation. Importantly, TOP2A is involved in various types of tumors, such as pancreatic cancer, breast cancer, lung cancer, glioblastoma, gastric cancer, colorectal cancer, hepatocellular carcinoma [15-22]. TOP2A is a key tumor-promoting gene frequently amplified in various human cancers and closely associated with cancer growth, metastasis, recurrence, and chemotherapy resistance [22]. However, if TOP2A is involved in resistance of HCC to regorafenib remains mysterious. Therefore, it is essential to investigate molecular mechanisms underlying drug resistance to regorafenib and to explore strategies to enhance efficacy of regorafenib in HCC. To fill in the gap in knowledge, we demonstrate, for the first time, that genetic and chemical inhibition of TOP2A reverses acquired resistance of human HCC to regorafenib. These results reveal a novel molecular mechanism underlying resistance to regorafenib in HCC and provide supporting evidence that TOP2A inhibitors may offer an attractive strategy for treating aggressive and regorafenib-resistant HCC.

Materials and methods

Cell culture, antibodies, and reagents

Human HCC cell line HepG2 was purchased from the American Type Culture Collection (ATCC; Manassas, VA, USA). Human HCC cell line Huh7 was purchased from Cell Bank of Type Culture Collection, Chinese Academy of Sciences (Shanghai, China). Cells were cultured at 37°C in Dulbecco's modified Eagle's medium (DMEM) (Gibco BRL, Grand Island, NY, USA) with 10% fresh fetal bovine serum. The corresponding sorafenib-resistant cells, named as Huh7-SR and HepG2-SR, were established by culturing parental cell lines in gradually increased concentrations of sorafenib. The concentration of sorafenib was slowly increased by 0.25 μM per week until stable growth in 10 μM sorafenib, as previously described [5, 22]. The antibodies (Abs) against TOP2A and cyclin D1 were purchased from ABclonal Biotech Co., Ltd. (Wuhan, China). The antibody against cleaved caspase-3 was from Cell Signaling Technology (Danvers, USA). Sorafenib was purchased from Jinan Trio Pharmatech Co., Ltd. (Jinan, China). The anti-β-actin, secondary Abs were purchased from Beijing Zhongshan Golden Bridge Biotechnology Co., Ltd. (Beijing, China). Regorafenib was purchased from Shanghai Biochempartner Co., Ltd. (Shanghai, China). Doxorubicin and epirubicin were purchased from Shanghai Biochempartner Co., Ltd. (Shanghai, China). Sorafenib, regorafenib, doxorubicin, and epirubicin were dissolved in dimethyl sulfoxide to make a stock solution. The (3,4,5-dimethylthiazol-2-yl)-2,5-diphenylterazolium bromide (MTT) was purchased from Solarbio, Co., Ltd. (Beijing, China).

Western blot

As described previously [5, 23], cells were treated as required, washed twice in cold PBS at pH 7.3 scraped, collected by centrifugation at 1500 rpm at 4°C. Equal amounts of protein extracts from tumor tissues of the animals. Briefly, the total proteins were extracted by lysis buffer (Beyotime Biotechnology; Beijing, China). The proteins were extracted using a Protein Extraction Kit (Bio Teke Corporation; Beijing, China) according to the manufacturer's instruc-

Table 1. siRNAs and their target genes used in the study

Genes	siRNA sequence	
	Forward: 5' to 3'	Reverse: 5' to 3'
TOP2A-1	AAACAGACAUGGAUGGAUAUU	PUAUCCAUCCAUGUCUGUUUUU
TOP2A-2	GAAAGAGUCCAUCAGAUUUUU	PAAAUCUGAUGGACUCUUUCUU
NC	UUCUCCGAACGUGUCACGUTT	ACGUGACACGUUCGGAGAATT

tions. The protein concentration of lysates was determined using protein assay kit (Bio-Rad; Richmond, CA, USA). The lysates were boiled in loading buffer for 5 min. Then, 30 μg-50 ug protein was subjected to sodium dodecyl sulfate (SDS) polyacrylamide gel electrophoresis. Resolved proteins were transferred onto polyvinylidene difluoride (PVDF) membranes. The membranes were blocked with 5% skim milk in TBST (Tris-buffered saline with 0.1% Tween 20) for 2 h and incubated with primary antibodies against TOP2A, cyclin D1, cleaved caspase-3, and β-actin, overnight at 4°C. After washing for 5 times with TBST, the membranes were incubated with the secondary Ab for 2 hours at room temperature. The membranes were washed for 5 times with TBST. The antibody-antigen complexes were observed by placing the membranes in a gel-imaging system and adding 200 μL/membrane of enhanced chemiluminescence (ECL) plus detection reagent (Pierce Chemical; Rockford, IL, USA). β-actin was used as loading control. All experiments were repeated thrice.

Cell viability assay

Cell viability was analyzed using MTT Assay. Briefly, Huh7, HepG2 and corresponding sorafenib-resistant cells were seeded in 96-well plates at a density of 3×10^3 cells/well overnight, subjected to different treatments (transfected with siTOP2A and/or incubated with 160 nM doxorubicin or gradually increasing concentrations of sorafenib or regorafenib or doxorubicin for 24 to 48 hours, respectively). After treatment, the supernatant was discarded. Culture medium was replaced by 200 μl fresh medium containing MTT solution (0.5 mg/ml) and incubated for another 4 h at 37°C. The purple formazan crystals were resuspended in 200 μl of DMSO. The absorbance was measured at 490 nm by a microplate reader. An optical density (OD) at 490 nm was measured. Cell viability (%) was calculated according to the formula: (experiment OD value-blank OD value)/(control OD value-blank OD value) × 100%.

siRNA transfection

The NCBI GenBank database was used to obtain gene sequence of TOP2A. The siRNAs were obtained using Invitrogen's RNAi express online design software, together with literature search. Then, double-stranded siRNA sequences for TOP2A and negative control siRNA were synthesized by GenePharma Pharmaceutical Technology Co., Ltd. (Shanghai, China). The siRNAs targeting TOP2A were named as siTOP2A-1, siTOP2A-2 whereas negative control siRNA as NC. All sequences and corresponding target genes were shown in **Table 1**. As described previously [5], after reached 70% to 90% confluence in 6-well plates, Huh7, HepG2, Huh7-SR, and HepG2-SR cells (5×10^5 cells per well) were incubated with siRNAs and NC by using equal volumes Lipofectamine 3000 (Thermo Fisher Scientific; Massachusetts, USA) diluted with Opti-MEM medium at a final concentration of 50 nM according to the manufacturer's instructions. After corresponding siRNAs were transferred into HCC cells for 24 to 48 hours, expression of the related proteins was analyzed by Western blot, and the cell viability was tested by MTT. All the above experiment was repeated three times.

Validation of the aberrant expression of TOP2A in HCC based TCGA datasets

The survival data were acquired in The Cancer Genome Atlas (TCGA) database and the overall survival (OS) was analyzed by the Kaplan-Meier Plotter.

Quantitative reverse transcription-polymerase chain reaction (qRT-PCR)

Huh7, HepG2 cells and the corresponding sorafenib-resistant cells Huh7-SR, HepG2-SR in the logarithmic phase were incubated with 0, 2.5, 5, or 7.5 μM sorafenib or regorafenib for 48 h. Total RNA was isolated from cells by Trizol Reagent from GE-NEWIZ Biotechnology Co., Ltd. (Suzhou, China) according to manufacturer's protocol. According to the primer design and synthesis technical standards, the TOP2A gene primer was designed and synthesized in

combination with literature, and GAPDH was used as an internal reference. The relevant sequences are shown as follows. With the primers targeting TOP2A (5'-GAAGTGTCACC-ATTGCAGCC-3'; 5'-TGTCTGGGCGGAGCAAAATA-3'), and GAPDH (5'-AAGAAGGTGGTGAAGCAG-GC-3'; 5-TCCACCACCCAGTTGCTGTA-3'). Briefly, as it has been described in detail [5], the extracted total RNA was reverse transcribed to synthesize cDNA using a reverse transcription kit. Then using the M × 3000P real-time PCR system (Stratagene, USA) to load the reverse transcription products obtained from the total RNA on the Taq Man array for quantitative reverse transcription-polymerase chain reaction (qRT-PCR). The specificity of amplification was confirmed by melting curves. Normalizing with the glyceraldehyde 3-phosphate dehydrogenase (GAPDH), relative mRNA levels of genes were calculated using the Ct values according to the formula: Ct value = $2^{-\Delta Ct}$[ΔCt = Ct target gene - Ct GAPDH], the Ct value is used to calculate the relative expression level of TOP2A mRNA. All the experiment repeated three times and then to calculate the average.

Colony formation assay

The sorafenib-resistant cells were seeded in the 6-well plates (10^3 cells/well) and incubated with 10 μM sorafenib or 10 μM regorafenib in DMEM medium. The incubation was ceased when the colony formation could be seen by naked eyes for about 14 days. The culture medium was then removed and washed with phosphate-buffered saline (PBS) three times. After that methanol was added into each well (2 ml/well) to fix the cells for 20 minutes. Later, the methanol was removed, and Crystal violet stain (2 mL) was added to incubate for 15 minutes. The cells were washed with flowing water and dried before the colonies were counted. The above experiments were repeated three times.

Wound healing assay

The cells were seeded in 6-well plates (3×10^5 cells/well) overnight. Three straight scratches were made across the surface of plates with a pipette tip, floating cells were removed by washing with PBS. Cells were divided into four groups (control, regorafenib, doxorubicin and regorafenib + doxorubicin), cultured in DMEM medium with 7.5 μM regorafenib in the regorafenib, and regorafenib + doxorubicin groups, 160 nM doxorubicin in the doxorubicin and regorafenib + doxorubicin group for 24 h. The images were taken with an inverted light microscope. Each assay was replicated three times.

Transwell migration and invasion assay

The migration and invasion assays were performed using Transwell chamber (Corning, NY, USA). HCC cells were divided into four groups (control, regorafenib, doxorubicin and regorafenib + doxorubicin). For migration assay, HCC cells were seeded into the upper chamber with serum-free medium (1×10^5 cells), and the bottom of the chamber contained the DMEM medium with 10% FBS. Both the upper or lower chamber contained 7.5 μM regorafenib and/or 160 nM doxorubicin as required. For invasion assay, the chamber was coated with Matrigel (BD Biosciences, Franklin Lakes, NJ, USA), and the other steps were similar to the migration assay. After migrated or invaded for 24 h, HCC cells were fixed with methanol for 20 minutes, washed three times with PBS, and then stained with crystal violet for 15 minutes, washed three times with PBS. Migrated and invaded HCC cells were then counted under an inverted light microscope. Migrated or invaded cells were quantified by counting the number of cells from 10 random fields at × 100 magnification. Each assay was replicated three times.

3D invasion

96 Well 3D Spheroid BME Cell Invasion (R&D systems, USA) more comprehensively and physiologically mimics in vivo scenario. Cell monolayers were washed with PBS, dissociated by Trypsin and neutralized with complete growth medium. Cell suspension was counted and diluted to 3×10^3/ml, to obtain spheroids of 300-500 μm in diameter at ≥ 4 days after seeded. The cell suspension was dispensed into 96-well round bottom plate and centrifuged at 200 × g for 5 min. The plate was transferred to an incubator (37°C, 5% CO_2, 95% humidity). After 4 days, tumor spheroid formation was visually confirmed and proceeded with 3D invasion. Invasion Matrix was thawed on ice overnight. 96-well plate containing 4-day old spheroids was placed on ice. 50 μl of Invasion Matrix was gently dispensed into each U-bottom well with 3 replicates for each condition. The plate was centrifuged at 4°C, 300 × g for 3 min,

then transferred to an incubator at 37°C, allowing the Invasion Matrix to solidify. After 1 h, 100 µl/well of complete growth medium was gently added. Invasion modulating agent (7.5 µM regorafenib or/and 160 nM doxorubicin) was applied to evaluate respective impact on cellular phenotype. After incubating at 37°C for 7 days, cell invasion was visualized at × 40 magnification using a microscope and quantitated with ImageJ.

Animal experiments

Six- to eight-week Male BALB/c-nu/nu immunodeficiency mice were obtained from Beijing Vital River Laboratory Animal Technology Co., Ltd. (Beijing, China), raised in the SPF-free environment. The animal experiments were had been approved by the Animal Ethic Committee of The Fourth Affiliated Hospital of Harbin Medical University (permit no. 2022-SCILL-SC-06) in line with National Laboratory Animal Regulations China Science and Technology Commission. Briefly, Huh7-SR cells (5×10^6)/100 µL PBS were subcutaneously inoculated into the right flank of the mice. The mice were randomized into four groups (n = 5/group): control, regorafenib, doxorubicin and regorafenib + doxorubicin. Regorafenib was administered to mice in the regorafenib and regorafenib + doxorubicin groups by gavage at a dose of 30 mg/kg, doxorubicin was intraperitoneally injected to mice at a dose of 5 mg/kg, and those in the control group received oral dimethyl sulfoxide and intraperitoneal injection of saline every three days. The tumor volume was calculated according to the longest and shortest vertical diameters using the following formula: $(a^2 \times b)/2$, where "a" represents the short axis, and "b" represents the long axis. Tumor volumes were measured every 3 days. At the end of the experiments, the tumors were harvested the weight and tumor size were measured.

Hematoxylin and eosin (H&E) and immunohistochemistry (IHC) staining

H&E and IHC were performed on liver tumor tissue sections from formalin-fixed and paraffin-embedded tissue blocks of xenograft models, respectively. Immunohistochemical staining was conducted on 4-µm FFPE unstained sections using antibodies against cyclin D1 and cleaved caspase-3. The tissue sections were deparaffinized by xylene and rehydrated in a descending ethanol. Slides were be subjected to antigen retrieval by ethylene diamine tetraacetic acid (EDTA) buffer (PH = 7.4) in boiled water for 30 minutes. Endogenous peroxidase activity was quenched with 3% H_2O_2 dissolved in methanol for 30 min, and incubated with primary antibody overnight at 4°C. After washed with PBST (phosphate buffered saline with 0.1% Tween 20), slides were incubated with secondary antibody for 30 min at room temperature, then washing the slides with PBST. Streptavidin horseradish peroxidase (HRP) for 30 min, staining with diaminobenzidine (DAB), and then counterstaining with hematoxylin. Finally, staining intensity and distribution of IHC were assessed by two senior pathologists in a blinded manner at The Fourth Affiliated Hospital of Harbin Medical University.

Statistical analysis

Statistical analyses were performed with SPSS (version 20), Data with normal distributions were represented by mean ± SD and analyzed using *t*-test or one-way ANOVA followed by Bonferroni post hoc. *P*-values ≤ 0.05 were considered to indicate statistical significance.

Results

HCC sorafenib-resistant cells are sensitive to regorafenib

As described previously [5, 23], sorafenib-resistant cells were established by culturing human HCC cell lines Huh7 and HepG2 in gradually increased concentrations of sorafenib. These cell lines were named as Huh7-SR and HepG2-SR. To investigate effects of sorafenib or regorafenib on parental HCC cells and sorafenib-resistant cells, different cell lines were incubated with serial concentrations of sorafenib or regorafenib for 48 h, and cell viability was assessed by MTT. As shown in **Figure 1A**, sorafenib inhibited viability of HepG2 and Huh7 cells, whereas with little effect on corresponding sorafenib-resistant cells HepG2-SR and Huh7-SR. By contrast, regorafenib exerted anticancer effects on HepG2-SR and Huh7-SR (**Figure 1B**). However, regorafenib (10 µM) exhibited suboptimal inhibition on viability of Huh7-SR and HepG2-SR (with an inhibitory rate of 56.3% and 55.5%, respectively) (**Figure 1B**). As expected, colony formation of Huh7-SR or

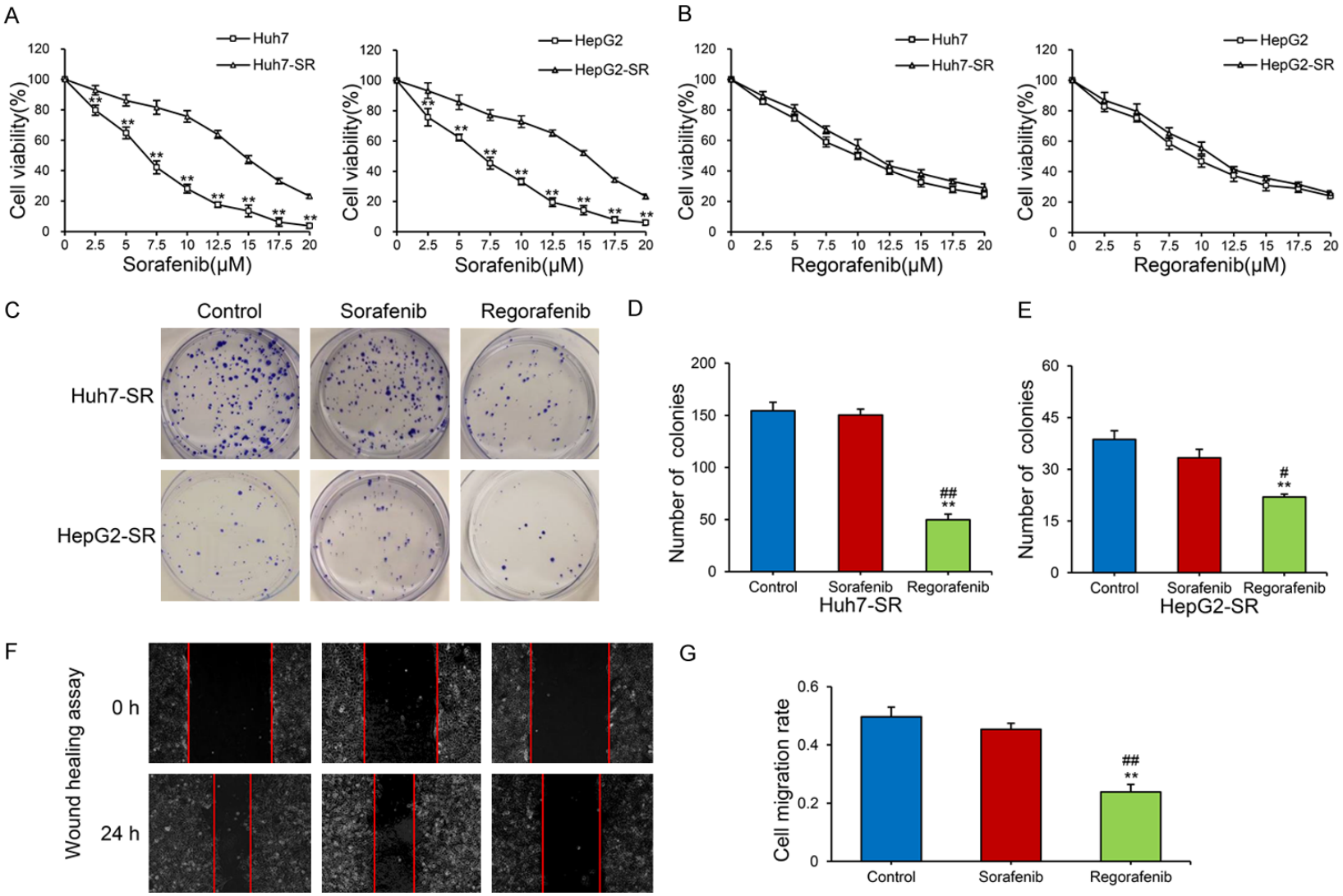

Figure 1. HCC sorafenib-resistant cells are sensitive to regorafenib. A, B. Sorafenib-resistant Huh7-SR and HepG2-SR as well as parental HepG2 and Huh7 were incubated with escalating concentrations of sorafenib or regorafenib for 48 hours. Cell viability was compared with corresponding untreated one. C-E. Colony formation assay to assess cell proliferation after incubating with 10 μM sorafenib or regorafenib for 15 days in Huh7-SR and HepG2-SR. F, G. Wound-healing assays (100 ×) to evaluate migration of sorafenib-resistant Huh7-SR after incubating with 10 μM sorafenib or regorafenib. $^{**}P < 0.01$ vs. the sorafenib-resistant cells or the untreated control group; $^{\#}P < 0.05$; $^{\#\#}P < 0.01$ vs. sorafenib group.

HepG2-SR was suppressed by regorafenib but not sorafenib (**Figure 1C-E**, $P < 0.05$). Similarly, invasion of Huh7-SR was decreased by regorafenib but not sorafenib (**Figure 1F**, **1G**, $P < 0.05$). Thus, sorafenib-resistant cells were sensitive to regorafenib.

TOP2A is involved in drug resistance to regorafenib

As described previously [13, 24, 25], TOP2A plays an important role in tumorigenesis and drug resistance. To investigate functions of latent genes in HCC, overall survival was analyzed using TCGA database. Interestingly, HCC patients with higher TOP2A expression had shorter overall survival (**Figure 2A**, $P < 0.01$). Then, expression profiling of TOP2A was detected in Huh7, HepG2 and corresponding sorafenib-resistant partners HepG2-SR and Huh7-SR cells. Compared with corresponding parental cells, TOP2A was downregulated in sorafenib-resistant Huh7-SR and HepG2-SR cells (**Figure 2B**, $P < 0.01$) as supported by qRT-PCR (**Figure 2C**, $P < 0.01$). Thus, sorafenib may downregulate TOP2A in HCC. Parental cells were incubated with escalating concertation of sorafenib, where TOP2A was down-regulated in a concentration-dependent manner (**Figure 2D**). Next, HCC parental cells and corresponding sorafenib-resistant cells were incubated with 0, 2.5, 5, and 7.5 μM regorafenib, respectively. Notably, sorafenib might suppress TOP2A, whereas regorafenib might upregulate TOP2A in a concentration-dependent manner ($P < 0.05$), as shown in **Figure 2D-F**. As shown in **Figure 2G**, **2H**, TOP2A was upregulated ($P < 0.05$) among sorafenib-resistant Huh7-SR and HepG2-SR cells in a concentration-dependent manner in response to regorafenib, however, corresponding parental cells treated with sorafenib exhibited an opposite trend ($P < 0.05$) supported by qRT-PCR. These findings indicated that TOP2A was involved in drug resistance to regorafenib.

TOP2A silencing enhances sensitivity to regorafenib in sorafenib-resistant HCC cells

To investigate roles of TOP2A in HCC sorafenib-resistance to regorafenib, two siRNAs were designed and synthesized to knock-down TOP2A. Both control siRNA- and TOP2A siRNA (siTOP2A) transfected Huh7-SR and HepG2-SR cell lines were incubated for 24 h. Compared with control, siTOP2A knocked down TOP2A protein expression in Huh7-SR and HepG2-SR cells (**Figure 3A**, **3B**, $P < 0.01$). Consequently, effects of siTOP2A in combination with regorafenib were analyzed. Huh7-SR and HepG2-SR as well as corresponding parental cells were transfected with control or siTOP2A for 24 h; subsequently incubated with increasing concentrations of regorafenib for another 48 h. To investigate if silencing of TOP2A could synergized with regorafenib to reduce cell viability, coefficient of drug interaction (CDI) was calculated as previously described [5]. The CDI of siRNA in combination with 2.5, 5, or 7.5 μM regorafenib, respectively, was less than 1, indicating marked synergistic effects (**Figure 3C**, **3D**; Table S1). The most optimized synergistic effect was exerted by siTOP2A in combination with 7.5 μM regorafenib, yielding CDIs of 0.682 and 0.694 for Huh7-SR and HepG2-SR, respectively (Table S1). Thus, combination treatment was used in subsequent experiments. Then, parental and sorafenib resistant cells were transfected with siTOP2A for 24 h and incubated with regorafenib for 24 h, 48 h, 72 h, respectively with CDI calculated (**Figure 3E**, **3F**; Table S2). The most optimized synergistic effect was exerted by incubating for 48 h, yielding CDIs of 0.696 and 0.684 for Huh7-SR and HepG2-SR, respectively (**Figure 3E**, **3F**; Table S2). Therefore, silencing TOP2A synergized with regorafenib could reduce viability of HepG2-SR and Huh7-SR cells in a dose- and time-dependent manner, similar to corresponding parental cells (**Figure 3C-F**; Table S2). To investigate roles of silencing TOP2A in combination with regorafenib, downstream genes were analyzed by Western blot (**Figure 3G**, **3H**). Silencing of TOP2A synergized with regorafenib to downregulate cyclin D1 and upregulate cleaved caspase-3 protein expression in sorafenib-resistant cells (**Figure 3G**, **3H**, $P < 0.05$). Thus, synergistic effect of regorafenib and silencing TOP2A was significantly on suppressing growth of HCC sorafenib-resistant cells and promoting apoptosis of HCC.

Inhibition of TOP2A synergizes with regorafenib to suppress cell viability, promote apoptosis, and increase sensitivity of sorafenib-resistant HCC cells to regorafenib in vitro

TOP2A is a target of anthracycline drugs, such as doxorubicin, epirubicin [26]. As previously described [27-29], doxorubicin interacts with DNA through intercalation and inhibition of

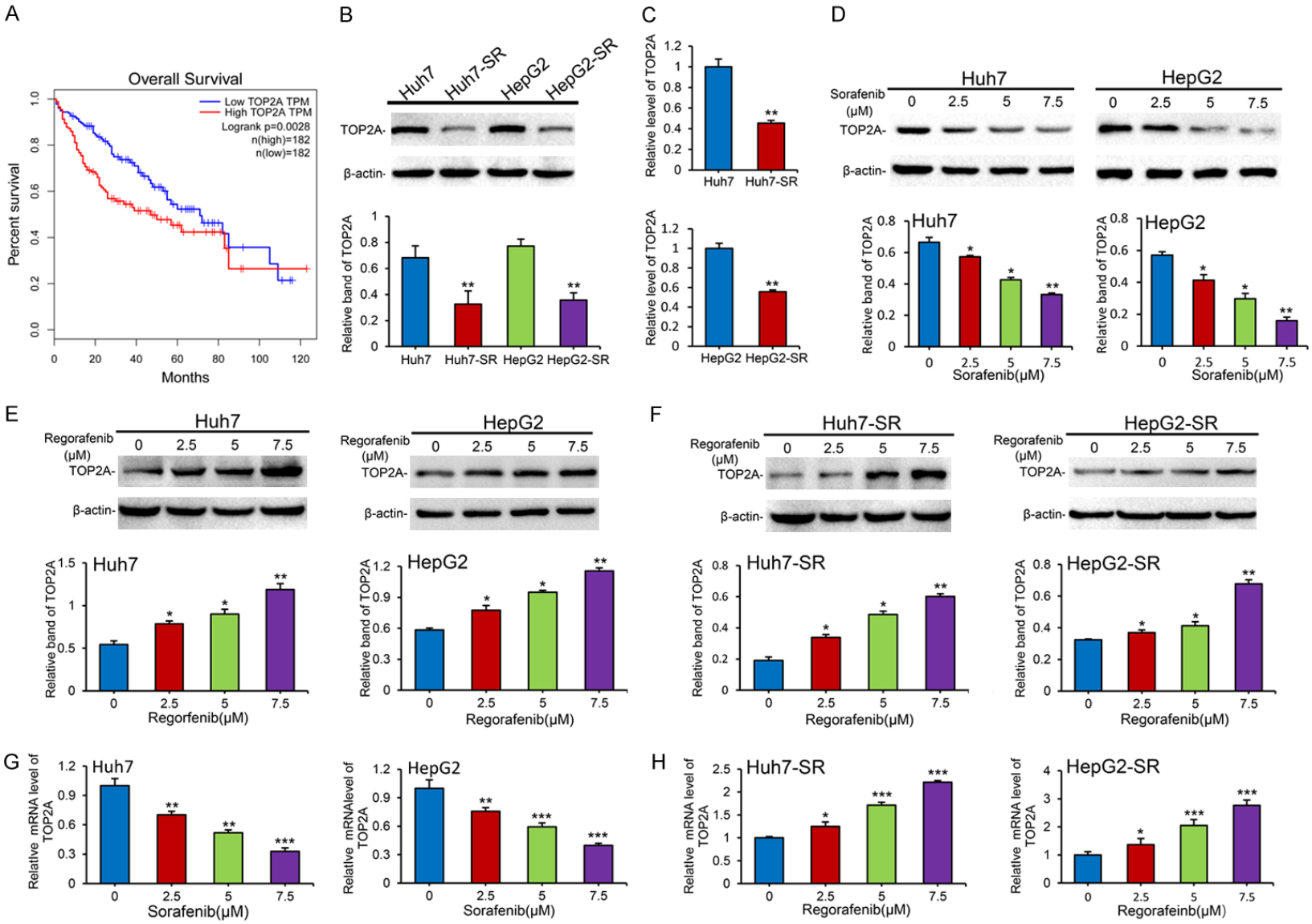

Figure 2. TOP2A is involved in drug resistance to regorafenib. (A) Kaplan-Meier curves for HCC patients with low vs. high expression of TOP2A using TCGA database. (B, C) TOP2A expression in sorafenib-resistant cell lines and corresponding parental cell lines detected by Western blot and normalized to β-actinin (B); or quantitative reverse transcription-polymerase chain reaction (qRT-PCR) and normalized to glyceraldehyde 3-phosphate dehydrogenase (GAPDH) (C). (D) Huh7 and HepG2 cells were incubated in gradually increased concentrations of sorafenib for 48 h. Expression of TOP2A was detected by Western blot. Density of each band was nor-

malized to that of β-actin. (E-H) Sorafenib-resistant Huh7-SR and HepG2-SR cells and corresponding parental cells were incubated with 0, 2.5, 5, 7.5 μM regorafenib for 48 h. The protein expression profiles were detected by Western blot. Density of each band was normalized to that of β-actin (E, F). Sorafenib-resistant HCC cells and parental cells were incubated with gradually increased concentrations of regorafenib or sorafenib for 48 h. TOP2A mRNA levels were measured by qRT-PCR and normalized against GAPDH. The relative TOP2A mRNA levels of cells treated with 0 μM sorafenib or regorafenib were normalized to 1 (G, H). $^{*}P < 0.05$; $^{**}P < 0.01$; and $^{***}P < 0.001$ vs. the sorafenib or regorafenib untreated cells.

macromolecular biosynthesis, resulting in double strand DNA breaks, then inhibiting progression of TOP2A and inducing subsequent apoptotic cell death of cancer cells [30, 31]. Therefore, effects of doxorubicin combined with regorafenib on viability and apoptosis of sorafenib-resistant as well as parental cells were examined. Huh7, HepG2 and corresponding sorafenib-resistant cells were incubated with regorafenib, doxorubicin or combination. Interestingly, inhibition of TOP2A by doxorubicin synergized with regorafenib could reduce viability in sorafenib-resistant cells as well as parental cells in a dose-dependent manner (**Figure 4A**, **4B**). The CDIs were calculated for HCC sorafenib-resistant and parental cells (Tables S3, S4, S5, S6). The CDIs for Huh7-SR and HepG2-SR cells and parental cells treated with 0, 80, 160, 320 nmol/L of doxorubicin in combination with regorafenib (0, 2.5, 5, 7.5 umol/L) were all less than 1, indicating a synergistic effect (Tables S3, S4, S5, S6). The most optimized synergistic effect was exerted by 160 nM doxorubicin in combination with 7.5 μM regorafenib, yielding CDIs of 0.679, 0.684, 0.681 and 0.698 for Huh7-SR, HepG2-SR, Huh7 and HepG2 cells, respectively. This combination was applied in subsequent experiments. As shown in **Figure 4C**, **4D**, doxorubicin synergized with regorafenib in inhibiting cell viability in a time-dependent manner. The CDI was 0.779, 0.646, and 0.752 for Huh7-SR, whereas 0.755, 0.660, 0.740 for HepG2-SR (Table S7), when incubated for 24, 48, or 72 h, respectively. The most optimized synergistic effect was exerted by incubating for 48 h. Then, effects of TOP2A inhibition on cell viability were supported by application of epirubicin, another TOP2A inhibitor. Epirubicin also exerted a significantly synergistic effect with regorafenib on inhibiting cell viability, with CDIs of 0.706 and 0.690 in Huh7-SR and HepG2-SR cells when incubating with 5 μM regorafenib and 160 nM epirubicin for 48 h, respectively, in time- and dose-dependent manners (Figures S1, S2, S3, S4; Tables S8, S9, S10, S11, S12). To confirm synergistic effects of regorafenib with doxorubicin on cell viability and apoptosis, sorafenib-resistant HCC cells were incubated with 7.5 μM regorafenib and/or 160 nM doxorubicin for 48 h, and then subjected to immunoblotting analyses. As shown in **Figure 4E**, regorafenib and doxorubicin exerted synergistic effect, as reflected by upregulation of cleaved caspase-3 whereas downregulation of cyclin D1 compared with either regorafenib or doxorubicin alone. Synergistic effect of regorafenib and doxorubicin was enough to suppress growth and promote apoptosis of HCC cells. The wound-healing assays also supported this notion (**Figure 4F**). As expected, migration and invasion of sorafenib-resistant HCC cells were significantly inhibited by regorafenib combined with doxorubicin ($P < 0.05$, **Figure 4G**). Furthermore, regorafenib combined with doxorubicin could also suppress 3D invasion and tumor sphere formation of HCC cells ($P < 0.05$, **Figures 4H**, S5).

Inhibition of TOP2A synergizes with regorafenib to enhance the antitumor activity of regorafenib in vivo

As described in Materials and Methods and our previous studies [5, 22], Huh7-SR cells were subcutaneously inoculated into the right flank. Mice were randomly divided into four groups accepting regorafenib, doxorubicin alone or combination treatment as required. As shown in **Figure 5A-C**, administration of regorafenib or doxorubicin into the mice reduced the size of tumors by 62.2% and 63.5%, respectively, and the combination therapy further significantly reduced by 90.4%, compared with the control group at 15 days after treatment, similar to tumor weight (**Figure 5B**, **5C**). The CDI was 0.709 for tumor volume and 0.729 for tumor weight, respectively, indicating a synergistically inhibitory effect of regorafenib and doxorubicin on growth of HCC tumor. The expression of downstream proteins was analyzed by Western blot (**Figure 5D**, **5E**). Consistently, doxorubicin and regorafenib combination downregulated

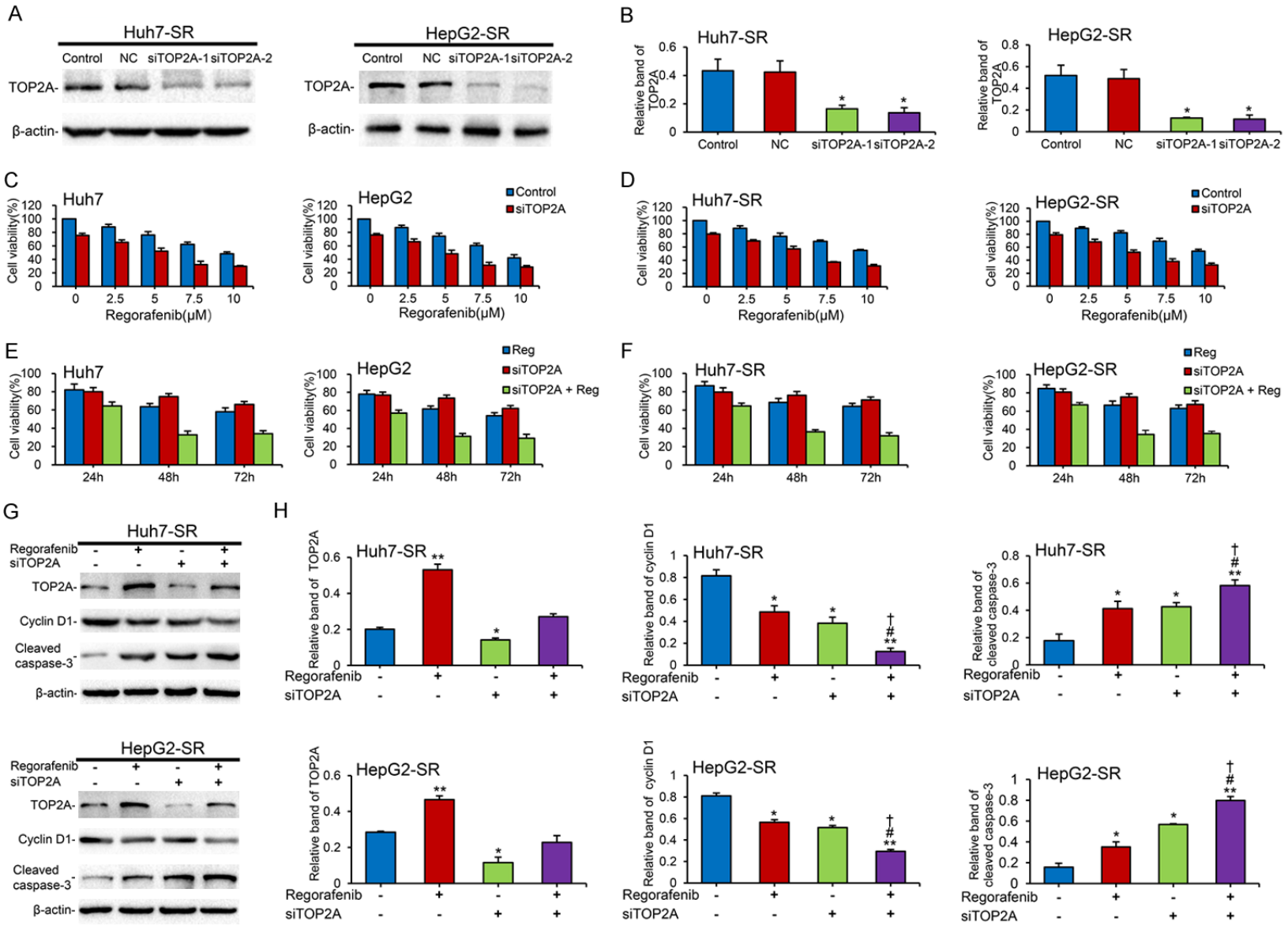

Figure 3. TOP2A silencing enhances sensitivity to regorafenib in sorafenib-resistant HCC cells. A, B. Sorafenib-resistant Huh7-SR and HepG2-SR cells were transfected with siTOP2A or negative control (NC) for 48 h. The corresponding un-transfected cells served as control. The protein expression profiles were detected by Western blot. Density of each band was normalized to that of β-actin. C, D. Huh7-SR and HepG2-SR cells and corresponding parental cells were transfected with siTOP2A for 24 h; subsequently incubated with increasing concentrations of regorafenib (Reg) for 48 h. Viability of transfected cells was normalized to control. E, F.

Sorafenib-resistant cells and parental cells were exposed to 7.5 μM regorafenib for different periods, after transfected with siTOP2A. Cell viability was normalized with corresponding control. G, H. Huh7-SR and HepG2-SR cells were transfected with siTOP2A for 24 h; subsequently incubated with 7.5 μM regorafenib for 48 h. Protein expression profiles were detected by Western blot. Density of each band was normalized to that of β-actin. $^{*}P < 0.05$; $^{**}P < 0.01$ compared siTOP2A or regorafenib to control. $^{\#}P < 0.05$; $^{\#\#}P < 0.01$ compared with regorafenib treated cells. $^{\dagger}P < 0.05$; $^{\dagger\dagger}P < 0.01$ compared with siTOP2A treated cells.

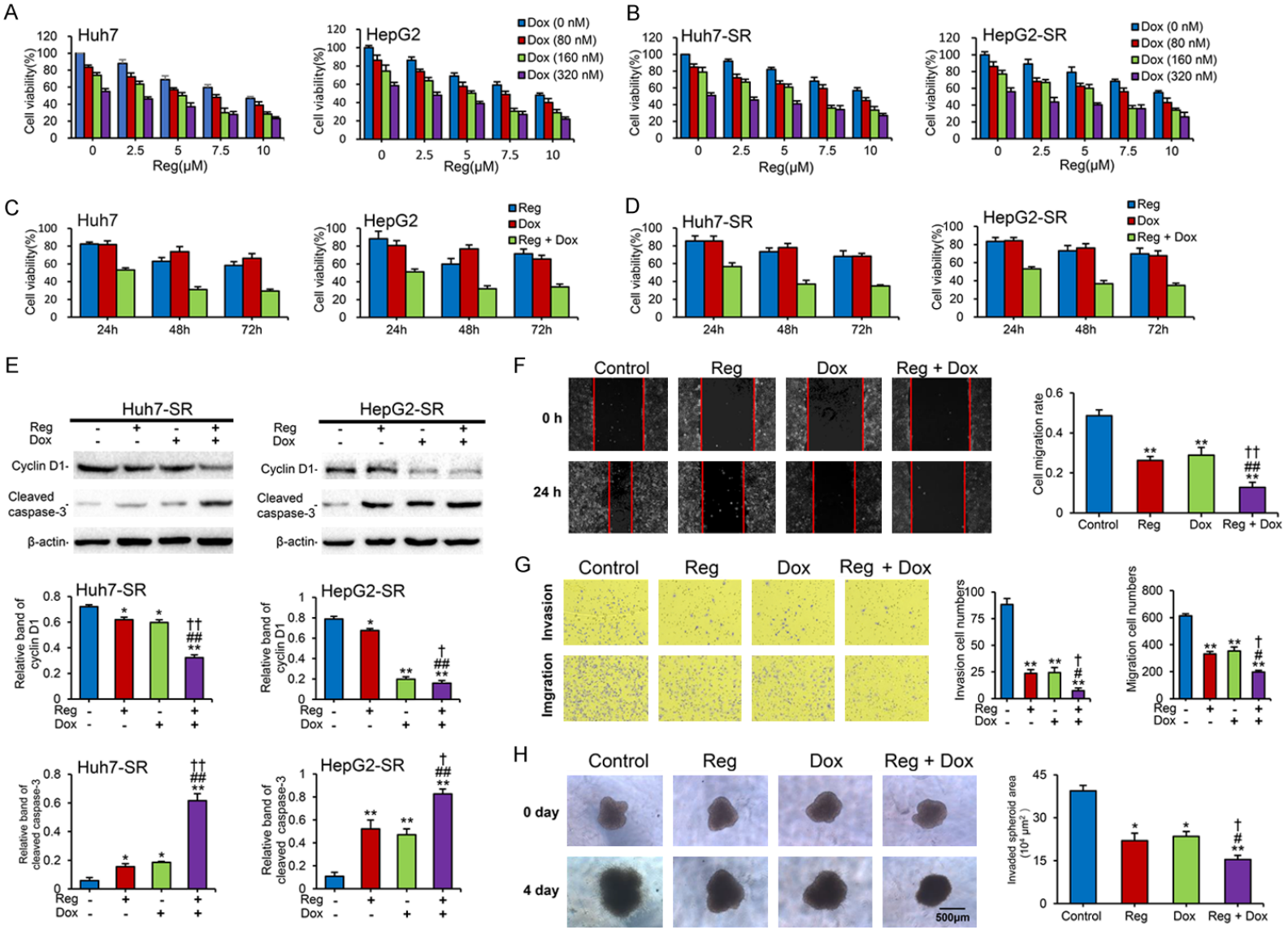

Figure 4. Inhibition of TOP2A synergizes with regorafenib to suppress cell viability, promote apoptosis, and strengthen sensitivity of sorafenib-resistant HCC cells to regorafenib in vitro. (A-D) HepG2-SR and Huh7-SR as well as corresponding parental cells were exposed to different concentrations of doxorubicin (Dox) or/and regorafenib (Reg) for 48 h (A, B); or incubated for different periods in the presence or absence of regorafenib (7.5 μM) and doxorubicin (160 nM) (C, D). Cell viability (%) was compared with control. (E) Huh7-SR and HepG2-SR cells were incubated with 7.5 μM regorafenib or/and 160 nM doxorubicin for 48 h. The protein expression profile of cyclin D1 and cleaved caspase-3 was detected by Western blot. Density of each band was normalized to that of β-actin. (F) Migration of sorafenib-resistant HCC cells was examined by Wound healing assay (100 ×). (G) Transwell assays to examine synergistic effects of doxorubicin with regorafenib on migration and invasion (100 ×). (H) Synergistic effects of doxorubicin and regorafenib on 3D invasion (40 ×). $^{*}P < 0.05$; $^{**}P < 0.01$; indicating a significant difference from untreated cells. $^{\#}P < 0.05$; $^{\#\#}P < 0.01$ compared with regorafenib treatment. $^{\dagger}P < 0.05$; $^{\dagger\dagger}P < 0.01$ compared with doxorubicin treated cells.

cyclin D1 and upregulated cleaved caspase-3 compared with either regorafenib or doxorubicin group. Then, H&E and immunohistochemistry staining of cyclin D1 and cleaved caspase-3 were applied to describe proliferation and apoptosis, respectively. The pathological findings were described in **Figures 5F-I** and S6A, S6B. Tumors in control group were composed of uniform big round cells and cleared-out cytoplasm cellularity. However, when treated with regorafenib or doxorubicin, a slight reduction in cellularity was showed. In regorafenib and doxorubicin groups, significant reduction in cellularity and extensive necrosis were common (**Figure 5F**, $P < 0.05$). Relative cell density in tumor was extensively reduced in regorafenib combined with doxorubicin treatment, compared to control or regorafenib alone (**Figure 5G**). The expression of cyclin D1, and cleaved caspase-3 were also detected in tumor tissues by immunohistochemistry staining. Consistent with our in vitro results, higher cleaved caspase-3 expression and lower cyclin D1 expression were detected in combination compared with regorafenib or doxorubicin alone (**Figure 5H**, **5I**).

Discussion

Drug resistance is an obstacle for HCC therapy. As previously reported [6, 10, 32, 33], drug resistance to regorafenib is characterized by a low response rate and reduced survival benefit, which poses a serious challenge due to a shortage of effective systemic treatments for HCC. Regorafenib was approved by USFDA in 2017 as a second-line treatment for patients with HCC. This was considered as a breath of fresh air for patients with sorafenib-resistant HCC. However, drug resistance to regorafenib emerges afterwards. Unfortunately, little is known about underlying mechanisms of resistance to regorafenib in HCC. Considering this dilemma that so far, no effective systemic therapy is available for HCC after failure of sorafenib and regorafenib therapy, it is urgent to develop reversal strategies. In this study, TOP2A is indicated to be a key regulator in mediating regorafenib resistance of HCC. Moreover, doxorubicin, a selective inhibitor of TOP2A, exhibits potential to rescue sensitivity of regorafenib-resistant HCC cells. Acquired drug resistance in HCC may be overcome by a combinatorial therapy including regorafenib with TOP2A inhibitor doxorubicin. In our study, roles of TOP2A were explored when parental HCC was treated with sorafenib, whereas sorafenib-resistant HCC cells treated with regorafenib. Sorafenib downregulates TOP2A whereas regorafenib upregulates TOP2A. TOP2A may provide a latent mechanism for sorafenib-resistant HCC cells refractory to regorafenib. Moreover, blocking TOP2A could enhance efficacy of regorafenib to combat HCC by promoting apoptosis and inhibiting proliferation. Regorafenib combination with TOP2A inhibitor could rescue sensitivity to regorafenib.

In cancer, TOP2A is widely overexpressed, and a high level of TOP2A correlates with poor clinical prognosis [15-22]. TOP2A expression is increased in proliferating cells (in G2/M phases of cell cycle) with active division [34]. TOP2A induces transient DNA double-strand breaks in proliferating cells to resolve DNA topological entanglements during chromosome condensation, replication, and segregation [35]. The basic characteristics of tumor cells are abnormal cell cycle and uncontrolled proliferation. Therefore, TOP2A in tumor pathogenesis has been widely studied [36, 37]. Previously, TOP2A was considered as a prognostic factor in patients with esophageal squamous cell carcinomas, breast cancer, clear cell renal cell carcinoma, nasopharyngeal carcinoma and HCC [14, 37-39]. It was reported that TOP2A was

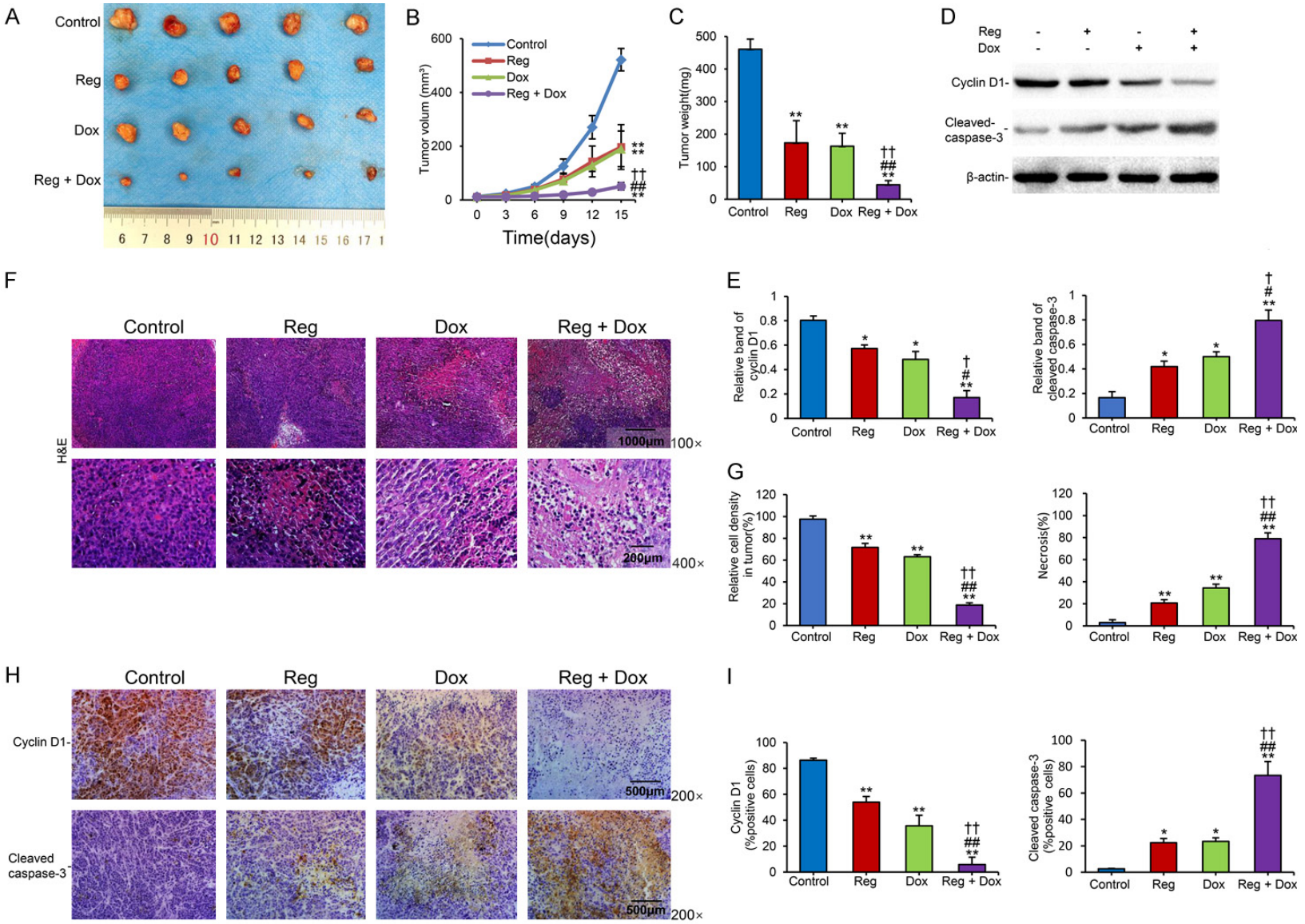

Figure 5. Inhibition of TOP2A synergizes with regorafenib to enhance the antitumor activity of regorafenib in vivo. (A-C) Subcutaneous xenografts were established. Mice received different treatments for 15 days. (A) Tumor images. (B) Tumor volume (mm^3) was recorded. (C) Tumors were harvested and weighed. (D, E) Expression of cyclin D1 and cleaved caspase-3 by Western blot. Density of each band was normalized to that of β-actin (E). (F-I) Hematoxylin and eosin (H&E) (magnification, upper × 100, lower × 400) and immunohistochemistry staining (magnification, × 200). $^{*}P < 0.05$; and $^{**}P < 0.01$. $^{\#}P < 0.05$; $^{\#\#}P < 0.01$ compared with regorafenib group. $^{\dagger}P < 0.05$; $^{\dagger\dagger}P < 0.01$ compared with doxorubicin treated group.

involved in the synthesis of membrane proteins with efflux functions, which eventually caused resistance to chemotherapy and targeted therapy. By inhibiting the activity of TOP2A, drug resistance could be reversed while apoptosis of cancer cells might be induced [40, 41]. In mammalian cells, function of TOP2A has been linked to posttranslational modification (acetylation, sumoylation or phosphorylation) [42, 43]. However, transcriptional and posttranscriptional mechanisms that control TOP2A expression are virtually unknown. To date, doxorubicin, TOP2A poison, functions by arresting TOP2A in cleavable complexes, resulting in double strand DNA breaks and subsequent apoptotic cell death of cancer cells. Doxorubicin is wildly used in breast cancer, leukemias, lymphomas and sarcoma [30].

Regorafenib inhibits stromal and angiogenic kinases VEGFR1, VEGFR2, VEGFR3, TIE2, FGFR-1 and PDGFRβ, oncogenic kinases KIT and RET, intracellular signaling kinases CRAF/RAF-1, wild-type and mutant BRAF, as well as PI3K/Akt and MAPK pathways [9, 33, 44]. These kinases play key roles in tumor neovascularization, stabilizing blood and lymphatic vessels as well as modulating tumor microenvironment, all of which contribute to oncogenesis and metastatic development [7, 9, 32]. Extensive studies have been conducted to explore mechanisms of drug-resistance to regorafenib. JAK-STAT, Notch1, epithelial-mesenchymal transition (EMT) and Keap/Nrf2 pathways have been implicated in resistance to regorafenib. For example, isomerase Pin1 inhibition could reverse EMT and reduce metastasis of regorafenib-resistant HCC cells via Gli1/Snail/E-cadherin pathway [31]. Notch-1 was essential in mediating regorafenib resistance. Thus, silencing of Notch-1 promoted regorafenib induced cell growth inhibition and cell cycle arrest [8]. In addition, SphK2/S1P mediates regorafenib resistance through activation of NF-κB and STAT3. Thus, inhibiting SphK2 could reduce regorafenib resistance of HCC cells [6]. Moreover, regorafenib tolerance was demonstrated to be associated with AKT/GSK3β regulated β-catenin [33].

It is well-known that caspase-3 is activated in both extrinsic and intrinsic apoptotic pathways. Notably, cyclin D1, a transcriptional co-regulator, controls cell cycle progression, regulates cell migration and invasion, promotes cell proliferation and inhibits apoptosis [45, 46]. Caspase-3 in the cytoplasm exists in the form of an inactive zymogen. The pro-apoptotic signals can lead to the cleavage and activation of caspase-3. Subsequently, active caspase-3 modulates cleavage of crucial cellular proteins and formation of apoptotic DNA fragmentation, and thus amplifies the protease cascade and cleavage reactions, which eventually results in cell death [45-47]. Previous studies have reported that TOP2A inhibitor causes apoptosis by upregulating caspase-3 [48, 49]. When DNA strand breaks reaching a critical level, enzyme/DNA complexes are induced, which cause the activation of stress-associated signaling pathways [50], characterized by upregulated γ-H2A.X, cleaved PARP-1, and activated caspase-3 as the hallmarks of apoptosis [51]. Afterwards, activated caspase-cascade leads to cell cycle arrest or apoptosis induction [36]. Recent studies showed that regorafenib could induce loss of mitochondrial membrane potential, as well as expression of active caspase-3 and caspase-8 [46, 52]. In addition, regorafenib triggered both intrinsic and extrinsic apoptotic pathways in colorectal cancer cells by activating caspase 3, 8 and 9. This result was attributed to inhibited PI3K/AKT/mTOR or MAPK signaling pathway [53, 54]. Inhibiting these pathways might block the phosphorylation of apoptosis signaling molecules or indirectly inhibit the activity of NF-κβ and suppress the transcriptional activation of antiapoptotic genes [47, 54].

Sorafenib executes anticancer activities against HCC, largely through inhibiting MAPK/ERK pathway and multiple tyrosine kinase receptors. However, sustained exposure to sorafenib could activate AKT, thus stimulating drug resistance to sorafenib as described in our precious studies in HCC cells [5, 23]. The present study indicated that sorafenib could downregulate TOP2A, however, regorafenib upregulates TOP2A. TOP2A may be a target of sorafenib. Although regorafenib is an oral tyrosine kinase inhibitor (TKI), similar to sorafenib, there are significant differences in molecular mechanisms from sorafenib. Firstly, regorafenib can inhibit the phosphorylation of AKT [33, 44, 56, 57]. However, when exposed to sorafenib, p-Akt could be upregulated [22, 32, 38, 40]. Then, p-GSK3β could be upregulated

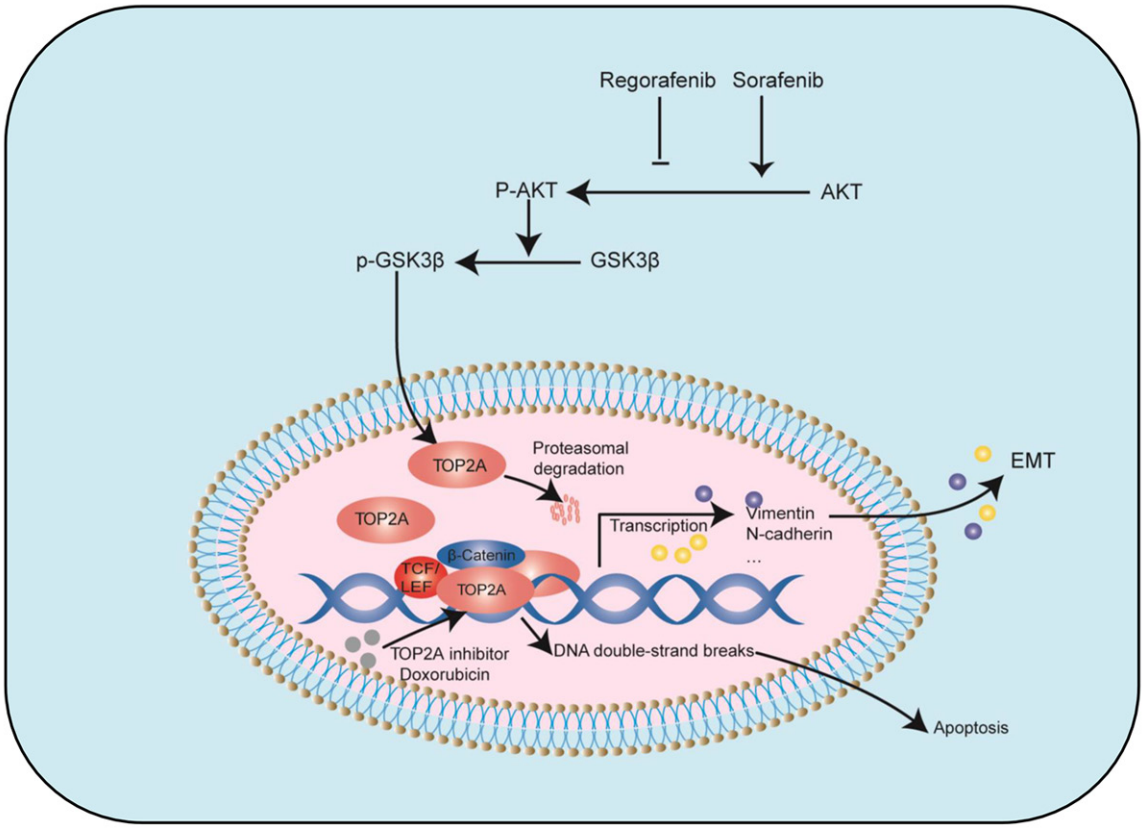

Figure 6. Schematic diagram depicting hypothesized roles of TOP2A in acquired resistance to regorafenib in HCC. →, positive regulation; ⊥, negative regulation or blockade.

by p-ATK via phosphorylation of serine residue of GSK3β [33, 54]. When treated with AKT pathway inhibitors (such as LY294002), GSK3β was upregulated [32]. Interestingly, a previous study reported that p-GSK3β was involved in degradation of TOP2A, leading to ubiquitin-dependent degradation in HCC. Accumulation of p-GSK3β could significantly downregulate TOP2A [40]. In addition, TOP2A could activate β-catenin pathway thus stimulating drug resistance to regorafenib in pancreatic cancer and colon cancer [15, 22]. TOP2A functions as a DNA-binding partner for TCF complex to interact with β-catenin, TCF4 and DNA through its C-terminus. TOP2A is involved in Wnt pathway, which controls T-cell fac-tor/lymphoid enhancer binding factor (TCF/LEF) gene transcription and dominates this self-renewing process. Persistent activation of Wnt-β-catenin pathway is common in carcinogenesis and drug-resistance in colorectal cancer, HCC and gastric cancer [5, 15, 57, 58] (**Figure 6**). In our study, knocking down of TOP2A synergizes with regorafenib promoted apoptosis and suppressed growth of sorafenib-resistant cells, reversing acquired drug resistance of regorafenib in HCC. Furthermore, when regorafenib was combined with TOP2A inhibitor doxorubicin, which functions by arresting TOP2A in cleavable complexes, resulting in double strand DNA breaks and subsequent apoptotic cell death of cancer cells [13, 31, 59], synergistic effects were observed both in vitro and in vivo. However, if silencing TOP2A could reverse acquired resistance to regorafenib via Wnt-β-catenin pathway through blocking EMT process needs further exploration (**Figure 6**).

Collectively, we have demonstrated that two-drug combination is highly effective against regorafenib-resistant HCC. We have illustrated, for the first time, that silencing TOP2A could reverse acquired drug resistance to regorafenib, possibly via inhibiting Wnt-β-catenin pathway, to rescue celluar sensitivity to regorafenib in HCC.

Acknowledgements

This project was supported by Spark Research Fund (Grant# HYDSYXH201904) of The Fourth Affiliated Hospital of Harbin Medical University.

Disclosure of conflict of interest

None.

Address correspondence to: Bo Zhai, Department of Surgical Oncology and Hepatobiliary Surgery, The Fourth Affiliated Hospital of Harbin Medical University, Harbin 150001, Heilongjiang, China. E-mail: zhaibo@hrbmu.edu.cn; Xiaoqun Dong, The Liver Research Center of Rhode Island Hospital/Lifespan; Department of Medicine, The Warren Alpert Medical School of Brown University, Providence, RI 02903, USA. E-mail: Xiaoqun_Dong@Brown.edu.cn

References

[1] Villanueva A. Hepatocellular carcinoma. N Engl J Med 2019; 380: 1450-1462.

[2] Sung H, Ferlay J, Siegel RL, Laversanne M, Soerjomataram I, Jemal A and Bray F. Global cancer statistics 2020: GLOBOCAN estimates of incidence and mortality worldwide for 36 cancers in 185 countries. CA Cancer J Clin 2021; 71: 209-249.

[3] Kim E and Viatour P. Hepatocellular carcinoma: old friends and new tricks. Exp Mol Med 2020; 52: 1898-1907.

[4] Moon H and Ro SW. MAPK/ERK signaling pathway in hepatocellular carcinoma. Cancers (Basel) 2021; 13: 3026.

[5] Zhu Q, Ren H, Li X, Qian B, Fan S, Hu F, Xu L and Zhai B. Silencing KIF14 reverses acquired resistance to sorafenib in hepatocellular carcinoma. Aging (Albany NY) 2020; 12: 22975-23003.

[6] Shi W, Zhang S, Ma D, Yan D, Zhang G, Cao Y, Wang Z, Wu J and Jiang C. Targeting SphK2 reverses acquired resistance of regorafenib in hepatocellular carcinoma. Front Oncol 2020; 10: 694.

[7] Wilhelm SM, Dumas J, Adnane L, Lynch M, Carter CA, Schutz G, Thierauch KH and Zopf D. Regorafenib (BAY 73-4506): a new oral multikinase inhibitor of angiogenic, stromal and oncogenic receptor tyrosine kinases with potent preclinical antitumor activity. Int J Cancer 2011; 129: 245-255.

[8] Mirone G, Perna S, Shukla A and Marfe G. Involvement of Notch-1 in resistance to regorafenib in colon cancer cells. J Cell Physiol 2016; 231: 1097-1105.

[9] Thillai K, Srikandarajah K and Ross P. Regorafenib as treatment for patients with advanced hepatocellular cancer. Future Oncol 2017; 13: 2223-2232.

[10] Bruix J, Qin S, Merle P, Granito A, Huang YH, Bodoky G, Pracht M, Yokosuka O, Rosmorduc O, Breder V, Gerolami R, Masi G, Ross PJ, Song T, Bronowicki JP, Ollivier-Hourmand I, Kudo M, Cheng AL, Llovet JM, Finn RS, LeBerre MA, Baumhauer A, Meinhardt G and Han G. Regorafenib for patients with hepatocellular carcinoma who progressed on sorafenib treatment (RESORCE): a randomised, double-blind, placebo-controlled, phase 3 trial. Lancet 2017; 389: 56-66.

[11] Chen T, Sun Y, Ji P, Kopetz S and Zhang W. Topoisomerase IIalpha in chromosome instability and personalized cancer therapy. Oncogene 2015; 34: 4019-4031.

[12] Lang AJ, Mirski SE, Cummings HJ, Yu Q, Gerlach JH and Cole SP. Structural organization of the human TOP2A and TOP2B genes. Gene 1998; 221: 255-266.

[13] Delgado JL, Hsieh CM, Chan NL and Hiasa H. Topoisomerases as anticancer targets. Biochem J 2018; 475: 373-398.

[14] Cao Y, Ke R, Wang S, Zhu X, Chen J, Huang C, Jiang Y and Lv L. DNA topoisomerase IIalpha and Ki67 are prognostic factors in patients with hepatocellular carcinoma. Oncol Lett 2017; 13: 4109-4116.

[15] Pei YF, Yin XM and Liu XQ. TOP2A induces malignant character of pancreatic cancer through activating beta-catenin signaling pathway. Biochim Biophys Acta Mol Basis Dis 2018; 1864: 197-207.

[16] Jandu H, Aluzaite K, Fogh L, Thrane SW, Noer JB, Proszek J, Do KN, Hansen SN, Damsgaard B, Nielsen SL, Stougaard M, Knudsen BR, Moreira J, Hamerlik P, Gajjar M, Smid M, Martens J, Foekens J, Pommier Y, Brunner N, Schrohl AS and Stenvang J. Molecular characterization of irinotecan (SN-38) resistant human breast cancer cell lines. BMC Cancer 2016; 16: 34.

[17] Cui Y, Pu R, Ye J, Huang H, Liao D, Yang Y, Chen W, Yao Y and He Y. LncRNA FAM230B promotes gastric cancer growth and metastasis by regulating the miR-27a-5p/TOP2A axis. Dig Dis Sci 2021; 66: 2637-2650.

[18] Ma W, Wang B, Zhang Y, Wang Z, Niu D, Chen S, Zhang Z, Shen N, Han W, Zhang X, Wei R and Wang C. Prognostic significance of TOP2A in non-small cell lung cancer revealed by bioinformatic analysis. Cancer Cell Int 2019; 19: 239.

[19] Song J, Ma Q, Hu M, Qian D, Wang B and He N. The inhibition of miR-144-3p on cell proliferation and metastasis by targeting TOP2A in HC-

MV-positive glioblastoma cells. Molecules 2018; 23: 3259.
[20] Tarpgaard LS, Qvortrup C, Nygard SB, Nielsen SL, Andersen DR, Jensen NF, Stenvang J, Detlefsen S, Brunner N and Pfeiffer P. A phase II study of epirubicin in oxaliplatin-resistant patients with metastatic colorectal cancer and TOP2A gene amplification. BMC Cancer 2016; 16: 91.
[21] Li N, Li L and Chen Y. The identification of core gene expression signature in hepatocellular carcinoma. Oxid Med Cell Longev 2018; 2018: 3478305.
[22] Zhou Q, Abraham AD, Li L, Babalmorad A, Bagby S, Arcaroli JJ, Hansen RJ, Valeriote FA, Gustafson DL, Schaack J, Messersmith WA and LaBarbera DV. Topoisomerase IIalpha mediates TCF-dependent epithelial-mesenchymal transition in colon cancer. Oncogene 2016; 35: 4990-4999.
[23] Zhai B, Hu F, Jiang X, Xu J, Zhao D, Liu B, Pan S, Dong X, Tan G, Wei Z, Qiao H, Jiang H and Sun X. Inhibition of Akt reverses the acquired resistance to sorafenib by switching protective autophagy to autophagic cell death in hepatocellular carcinoma. Mol Cancer Ther 2014; 13: 1589-1598.
[24] El-Deiry WS, Vijayvergia N, Xiu J, Scicchitano A, Lim B, Yee NS, Harvey HA, Gatalica Z and Reddy S. Molecular profiling of 6,892 colorectal cancer samples suggests different possible treatment options specific to metastatic sites. Cancer Biol Ther 2015; 16: 1726-1737.
[25] An X, Xu F, Luo R, Zheng Q, Lu J, Yang Y, Qin T, Yuan Z, Shi Y, Jiang W and Wang S. The prognostic significance of topoisomerase II alpha protein in early stage luminal breast cancer. BMC Cancer 2018; 18: 331.
[26] Yang Z, Liu Y, Shi C, Zhang Y, Lv R, Zhang R, Wang Q and Wang Y. Suppression of PTEN/AKT signaling decreases the expression of TUBB3 and TOP2A with subsequent inhibition of cell growth and induction of apoptosis in human breast cancer MCF-7 cells via ATP and caspase-3 signaling pathways. Oncol Rep 2017; 37: 1011-1019.
[27] Patel AG and Kaufmann SH. How does doxorubicin work? Elife 2012; 1: e00387.
[28] Riccio AA, Schellenberg MJ and Williams RS. Molecular mechanisms of topoisomerase 2 DNA-protein crosslink resolution. Cell Mol Life Sci 2020; 77: 81-91.
[29] Seoane JA, Kirkland JG, Caswell-Jin JL, Crabtree GR and Curtis C. Chromatin regulators mediate anthracycline sensitivity in breast cancer. Nat Med 2019; 25: 1721-1727.
[30] Turner JG, Dawson JL, Grant S, Shain KH, Dalton WS, Dai Y, Meads M, Baz R, Kauffman M, Shacham S and Sullivan DM. Treatment of acquired drug resistance in multiple myeloma by combination therapy with XPO1 and topoisomerase II inhibitors. J Hematol Oncol 2016; 9: 73.
[31] Giles GI and Sharma RP. Topoisomerase enzymes as therapeutic targets for cancer chemotherapy. Med Chem 2005; 1: 383-394.
[32] Wang J, Zhang N, Han Q, Lu W, Wang L, Yang D, Zheng M, Zhang Z, Liu H, Lee TH, Zhou XZ and Lu KP. Pin1 inhibition reverses the acquired resistance of human hepatocellular carcinoma cells to regorafenib via the Gli1/Snail/E-cadherin pathway. Cancer Lett 2019; 444: 82-93.
[33] Ou B, Cheng X, Xu Z, Chen C, Shen X, Zhao J and Lu A. A positive feedback loop of beta-catenin/CCR2 axis promotes regorafenib resistance in colorectal cancer. Cell Death Dis 2019; 10: 643.
[34] Bhosle J, Kiakos K, Porter AC, Wu J, Makris A, Hartley JA and Hochhauser D. Treatment with gefitinib or lapatinib induces drug resistance through downregulation of topoisomerase IIalpha expression. Mol Cancer Ther 2013; 12: 2897-2908.
[35] Elton TS, Ozer HG and Yalowich JC. Effects of DNA topoisomerase IIalpha splice variants on acquired drug resistance. Cancer Drug Resist 2020; 3: 161-170.
[36] Muller L, Schutte LRF, Bucksteeg D, Alfke J, Uebel T and Esselen M. Topoisomerase poisoning by the flavonoid nevadensin triggers DNA damage and apoptosis in human colon carcinoma HT29 cells. Arch Toxicol 2021; 95: 3787-3802.
[37] Parker AS, Eckel-Passow JE, Serie D, Hilton T, Parasramka M, Joseph RW, Wu KJ, Cheville JC and Leibovich BC. Higher expression of topoisomerase II alpha is an independent marker of increased risk of cancer-specific death in patients with clear cell renal cell carcinoma. Eur Urol 2014; 66: 929-935.
[38] Xu XL, Zheng WH, Fu ZX, Li ZP, Xie HX, Li XX, Jiang LH, Wang Y, Zhu SM and Mao WM. Topo2A as a prognostic biomarker for patients with resectable esophageal squamous cell carcinomas. Med Oncol 2015; 32: 396.
[39] Mrklic I, Pogorelic Z, Capkun V and Tomic S. Expression of topoisomerase II-alpha in triple negative breast cancer. Appl Immunohistochem Mol Morphol 2014; 22: 182-187.
[40] Jun KY, Park SE, Liang JL, Jahng Y and Kwon Y. Benzo[b]tryptanthrin inhibits MDR1, topoisomerase activity, and reverses adriamycin resistance in breast cancer cells. ChemMedChem 2015; 10: 827-835.
[41] Cao B, Chen H, Gao Y, Niu C, Zhang Y and Li L. CIP-36, a novel topoisomerase II-targeting agent, induces the apoptosis of multidrug-re-

sistant cancer cells in vitro. Int J Mol Med 2015; 35: 771-776.
[42] Chen MC, Chen CH, Chuang HC, Kulp SK, Teng CM and Chen CS. Novel mechanism by which histone deacetylase inhibitors facilitate topoisomerase IIalpha degradation in hepatocellular carcinoma cells. Hepatology 2011; 53: 148-159.
[43] Srikantan S, Abdelmohsen K, Lee EK, Tominaga K, Subaran SS, Kuwano Y, Kulshrestha R, Panchakshari R, Kim HH, Yang X, Martindale JL, Marasa BS, Kim MM, Wersto RP, Indig FE, Chowdhury D and Gorospe M. Translational control of TOP2A influences doxorubicin efficacy. Mol Cell Biol 2011; 31: 3790-3801.
[44] Subramonian D, Phanhthilath N, Rinehardt H, Flynn S, Huo Y, Zhang J, Messer K, Mo Q, Huang S, Lesperance J and Zage PE. Regorafenib is effective against neuroblastoma in vitro and in vivo and inhibits the RAS/MAPK, PI3K/Akt/mTOR and Fos/Jun pathways. Br J Cancer 2020; 123: 568-579.
[45] Hsu FT, Sun CC, Wu CH, Lee YJ, Chiang CH and Wang WS. Regorafenib induces apoptosis and inhibits metastatic potential of human bladder carcinoma cells. Anticancer Res 2017; 37: 4919-4926.
[46] Pan PJ, Liu YC and Hsu FT. Protein kinase B and extracellular signal-regulated kinase inactivation is associated with regorafenib-induced inhibition of osteosarcoma progression in vitro and in vivo. J Clin Med 2019; 8: 900.
[47] Jiang M, Qi L, Li L and Li Y. The caspase-3/GSDME signal pathway as a switch between apoptosis and pyroptosis in cancer. Cell Death Discov 2020; 6: 112.
[48] Kamal A, Suresh P, Ramaiah MJ, Srinivasa Reddy T, Kapavarapu RK, Rao BN, Imthiajali S, Lakshminarayan Reddy T, Pushpavalli SN, Shankaraiah N and Pal-Bhadra M. 4beta-[4'-(1-(Aryl)ureido)benzamide]podophyllotoxins as DNA topoisomerase I and IIalpha inhibitors and apoptosis inducing agents. Bioorg Med Chem 2013; 21: 5198-5208.
[49] Chen S, Ren Z, Yu D, Ning B and Guo L. DNA damage-induced apoptosis and mitogen-activated protein kinase pathway contribute to the toxicity of dronedarone in hepatic cells. Environ Mol Mutagen 2018; 59: 278-289.
[50] Wong RS. Apoptosis in cancer: from pathogenesis to treatment. J Exp Clin Cancer Res 2011; 30: 87.
[51] Monger A, Boonmuen N, Suksen K, Saeeng R, Kasemsuk T, Piyachaturawat P, Saengsawang W and Chairoungdua A. Inhibition of topoisomerase IIalpha and induction of apoptosis in gastric cancer cells by 19-triisopropyl andrographolide. Asian Pac J Cancer Prev 2017; 18: 2845-2851.
[52] Yu CC, Huang SY, Chang SF, Liao KF and Chiu SC. The synergistic anti-cancer effects of NVP-BEZ235 and regorafenib in hepatocellular carcinoma. Molecules 2020; 25: 2454.
[53] Liu YC, Tsai JJ, Weng YS and Hsu FT. Regorafenib suppresses epidermal growth factor receptor signaling-modulated progression of colorectal cancer. Biomed Pharmacother 2020; 128: 110319.
[54] Salahuddin MM, Omran GA, Helmy MW and Houssen ME. Effect of regorafenib on P2X7 receptor expression and different oncogenic signaling pathways in a human breast cancer cell line: a potential of new insight of the antitumor effects of regorafenib. Curr Issues Mol Biol 2021; 43: 2199-2209.
[55] Chen X, Yan X and Guo L. Inhibitory effect of Patrinia on BRL-3A cell apoptosis through the TLR4/PI3K/AKT/GSK3beta and TLR4/P38/JNK signaling pathways. Mol Med Rep 2018; 17: 5344-5349.
[56] Duda P, Akula SM, Abrams SL, Steelman LS, Martelli AM, Cocco L, Ratti S, Candido S, Libra M, Montalto G, Cervello M, Gizak A, Rakus D and McCubrey JA. Targeting GSK3 and associated signaling pathways involved in cancer. Cells 2020; 9: 1110.
[57] Vilchez V, Turcios L, Marti F and Gedaly R. Targeting Wnt/beta-catenin pathway in hepatocellular carcinoma treatment. World J Gastroenterol 2016; 22: 823-832.
[58] Huang L, Shitashige M, Satow R, Honda K, Ono M, Yun J, Tomida A, Tsuruo T, Hirohashi S and Yamada T. Functional interaction of DNA topoisomerase IIalpha with the beta-catenin and T-cell factor-4 complex. Gastroenterology 2007; 133: 1569-1578.
[59] Godel M, Morena D, Ananthanarayanan P, Buondonno I, Ferrero G, Hattinger CM, Di Nicolantonio F, Serra M, Taulli R, Cordero F, Riganti C and Kopecka J. Small nucleolar RNAs determine resistance to doxorubicin in human osteosarcoma. Int J Mol Sci 2020; 21: 4500.

Supplementary materials and methods

Mammosphere formation

300 μl of Matrigel was spread evenly to each well of a 24-well plate on ice. The plate was centrifuged at 4°C, 300 × g; and immediately incubated at 37°C, in 5% CO_2 for 30 min. Single-cells were suspended in corresponding medium with 10% Matrigel (2000 cells/400 μl) and seeded on Matrigel. Cells were allowed to attach to Matrigel for 3 h. Then medium was carefully removed, replaced with fresh one containing 10% Matrigel and incubated for 1 h, corresponding culture medium as required was added. Fresh medium containing Matrigel and modulating agent (7.5 μM regorafenib or/and 160 Nm doxorubicin) was changed every 2 days. Mammospheres formed after 6 days were evaluated in terms of size and number by light microscopy × 40 magnification. All experiments were performed in triplicate wells for each condition.

Table S1. The CDIs of siTOP2A in combination with Regorafenib in HCC cells

Regorafenib (μM)	2.5	5	7.5	10
siTOP2A (Huh7)	0.984	0.908	0.685	0.812
siTOP2A (Huh7-SR)	0.984	0.943	0.682	0.720
siTOP2A (HepG2)	0.996	0.851	0.680	0.883
siTOP2A (HepG2-SR)	0.965	0.801	0.694	0.759

Abbreviations: CDI, coefficient of drug interaction. siTOP2A, topoisomerase IIα siRNA.

Table S2. The CDIs of siTOP2A in combination with 7.5 μM Regorafenib in HCC cells

CDI	24 h	48 h	72 h
siTOP2A (Huh7)	0.982	0.691	0.888
siTOP2A (Huh7-SR)	0.936	0.696	0.704
siTOP2A (HepG2)	0.950	0.690	0.865
siTOP2A (HepG2-SR)	0.975	0.684	0.837

Abbreviations: CDI, coefficient of drug interaction. siTOP2A, topoisomerase IIα siRNA.

Table S3. The CDIs of doxorubicin in combination with regorafenib in Huh7 cells

CDI	Reg (2.5 μM)	Reg (5 μM)	Reg (7.5 μM)	Reg (10 μM)
Dox (80 nM)	0.983	0.989	0.965	0.992
Dox (160 nM)	0.977	0.983	0.681	0.824
Dox (320 nM)	0.954	0.976	0.855	0.895

Abbreviations: CDI, coefficient of drug interaction; Reg, regorafenib; Dox, doxorubicin.

Table S4. The CDIs of doxorubicin in combination with regorafenib in HepG2 cells

CDI	Reg (2.5 μM)	Reg (5 μM)	Reg (7.5 μM)	Reg (10 μM)
Dox (80 nM)	0.992	0.970	0.958	0.967
Dox (160 nM)	0.998	0.987	0.698	0.816
Dox (320 nM)	0.950	0.964	0.781	0.783

Abbreviations: CDI, coefficient of drug interaction; Reg, regorafenib; Dox, doxorubicin.

Table S5. The CDIs of doxorubicin in combination with regorafenib in Huh7-SR cells

CDI	Reg (2.5 μM)	Reg (5 μM)	Reg (7.5 μM)	Reg (10 μM)
Dox (80 nM)	0.982	0.992	0.987	0.991
Dox (160 nM)	0.934	0.954	0.679	0.848
Dox (320 nM)	0.977	0.982	0.965	0.937

Abbreviations: CDI, coefficient of drug interaction; Reg, regorafenib; Dox, doxorubicin.

Table S6. The CDIs of doxorubicin in combination with regorafenib in HepG2-SR cells

CDI	Reg (2.5 μM)	Reg (5 μM)	Reg (7.5 μM)	Reg (10 μM)
Dox (80 nM)	0.890	0.921	0.951	0.911
Dox (160 nM)	0.978	0.986	0.684	0.805
Dox (320 nM)	0.879	0.910	0.939	0.848

Abbreviations: CDI, coefficient of drug interaction; Reg, regorafenib; Dox, doxorubicin.

Table S7. The CDIs of 160 nM doxorubicin in combination with 7.5 μM Regorafenib in HCC cells

CDI	24 h	48 h	72 h
Huh7	0.791	0.672	0.764
HepG2	0.718	0.699	0.735
Huh7-SR	0.779	0.646	0.752
HepG2-SR	0.755	0.660	0.740

Abbreviations: CDI, coefficient of drug interaction.

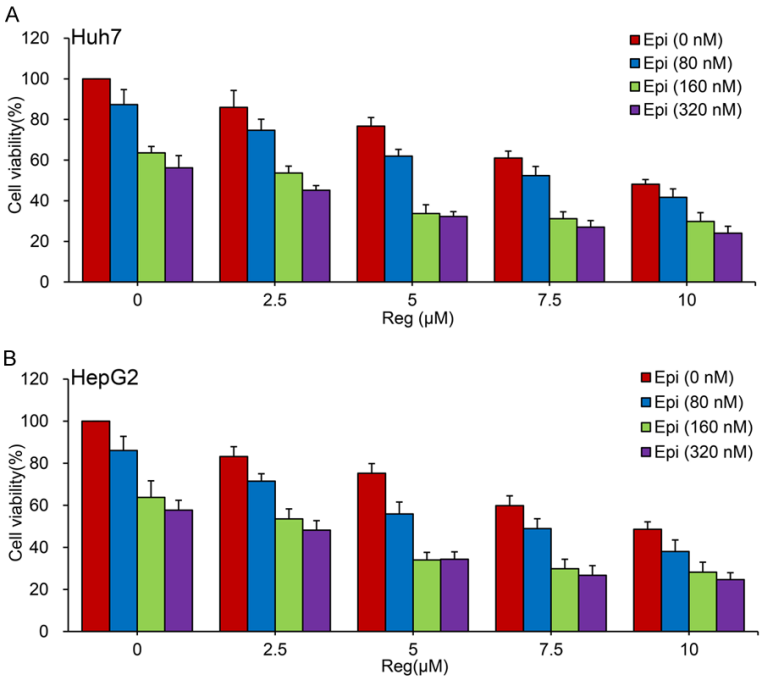

Figure S1. The effect of TOP2A inhibitors combined with regorafenib on cell viability and proliferation. A, B. Huh7 and HepG2 cells were exposed for 48 hours to different concentrations of epirubicin (Epi) or/and regorafenib (Reg).

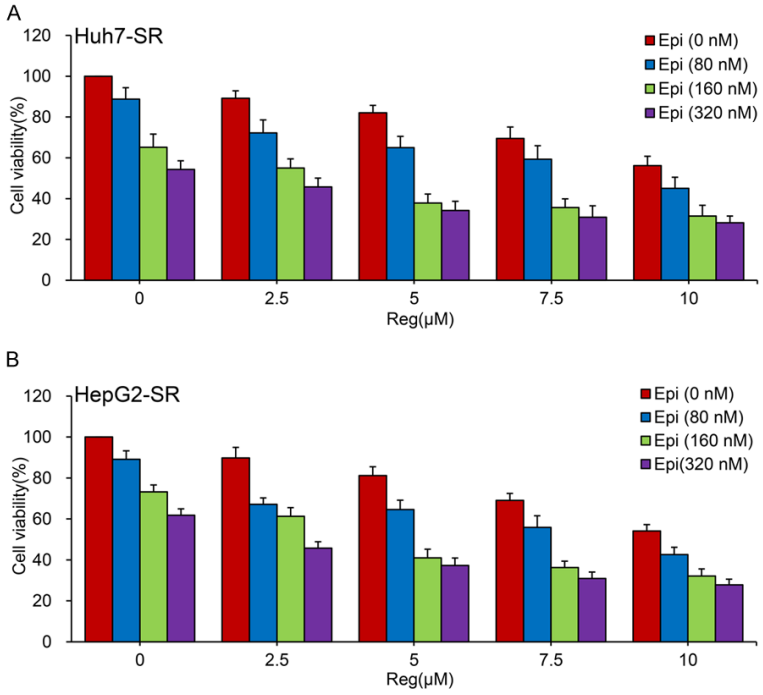

Figure S2. The effect of TOP2A inhibitors combined with regorafenib on cell viability and proliferation. A, B. Huh7-SR and HepG2-SR cells were exposed for 48 hours to different concentrations of epirubicin (Epi) or/and regorafenib (Reg).

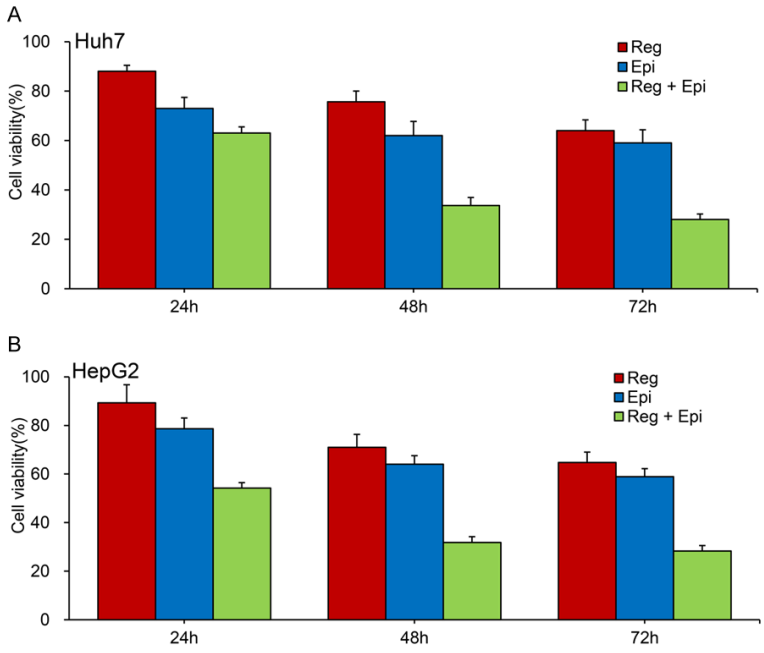

Figure S3. The effect of TOP2A inhibitors combined with regorafenib on cell viability and proliferation. A, B. Huh7 and HepG2 cells were incubating for different periods, in the presence or absence of regorafenib (Reg, 5 μM) and epirubicin (Epi, 160 nM).

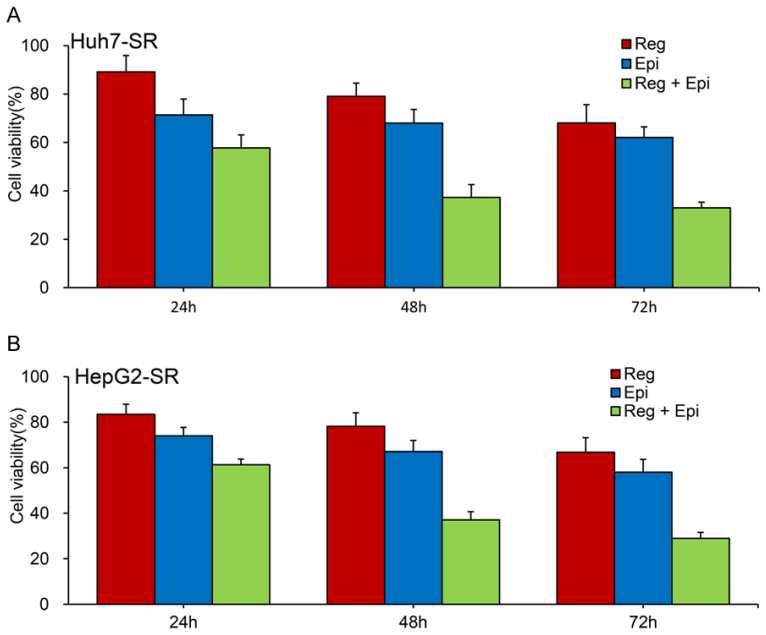

Figure S4. The effect of TOP2A inhibitors combined with regorafenib on cell viability and proliferation. A, B. Huh7-SR and HepG2-SR cells were incubating for different periods, in the presence or absence of regorafenib (Reg, 5 μM) and epirubicin (Epi, 160 nM).

Table S8. The CDIs of epirubicin in combination with regorafenib in Huh7 cells

CDI	Reg (2.5 μM)	Reg (5 μM)	Reg (7.5 μM)	Reg (10 μM)
Epi (80 nM)	0.995	0.926	0.984	0.994
Epi (160 nM)	0.982	0.691	0.805	0.976
Epi (320 nM)	0.934	0.749	0.788	0.888

Abbreviations: CDI, coefficient of drug interaction; Reg, regorafenib; Epi, eipirubicin.

Table S9. The CDIs of epirubicin in combination with regorafenib in HepG2 cells

CDI	Reg (2.5 μM)	Reg (5 μM)	Reg (7.5 μM)	Reg (10 μM)
Epi (80 nM)	0.998	0.864	0.951	0.909
Epi (160 nM)	1.009	0.710	0.783	0.911
Epi (320 nM)	1.003	0.790	0.774	0.877

Abbreviations: CDI, coefficient of drug interaction; Reg, regorafenib; Epi, eipirubicin.

Table S10. The CDIs of epirubicin in combination with regorafenib in Huh7-SR cells

CDI	Reg (2.5 μM)	Reg (5 μM)	Reg (7.5 μM)	Reg (10 μM)
Epi (80 nM)	0.911	0.892	0.961	0.902
Epi (160 nM)	0.946	0.706	0.786	0.860
Epi (320 nM)	0.944	0.767	0.819	0.921

Abbreviations: CDI, coefficient of drug interaction; Reg, regorafenib; Epi, eipirubicin.

Table S11. The CDIs of epirubicin in combination with regorafenib in HepG2-SR cells

CDI	Reg (2.5 μM)	Reg (5 μM)	Reg (7.5 μM)	Reg (10 μM)
Epi (80 nM)	0.839	0.892	0.908	0.884
Epi (160 nM)	0.933	0.690	0.718	0.811
Epi (320 nM)	0.824	0.744	0.724	0.831

Abbreviations: CDI, coefficient of drug interaction; Reg, regorafenib; Epi, eipirubicin.

Table S12. The CDIs of 160 nM epirubicin in combination with 5 μM Regorafenib in HCC cells

CDI	24 h	48 h	72 h
Huh7	0.981	0.718	0.742
HepG2	0.772	0.700	0.743
Huh7-SR	0.908	0.693	0.780
HepG2-SR	0.993	0.707	0.749

Abbreviations: CDI, coefficient of drug interaction.

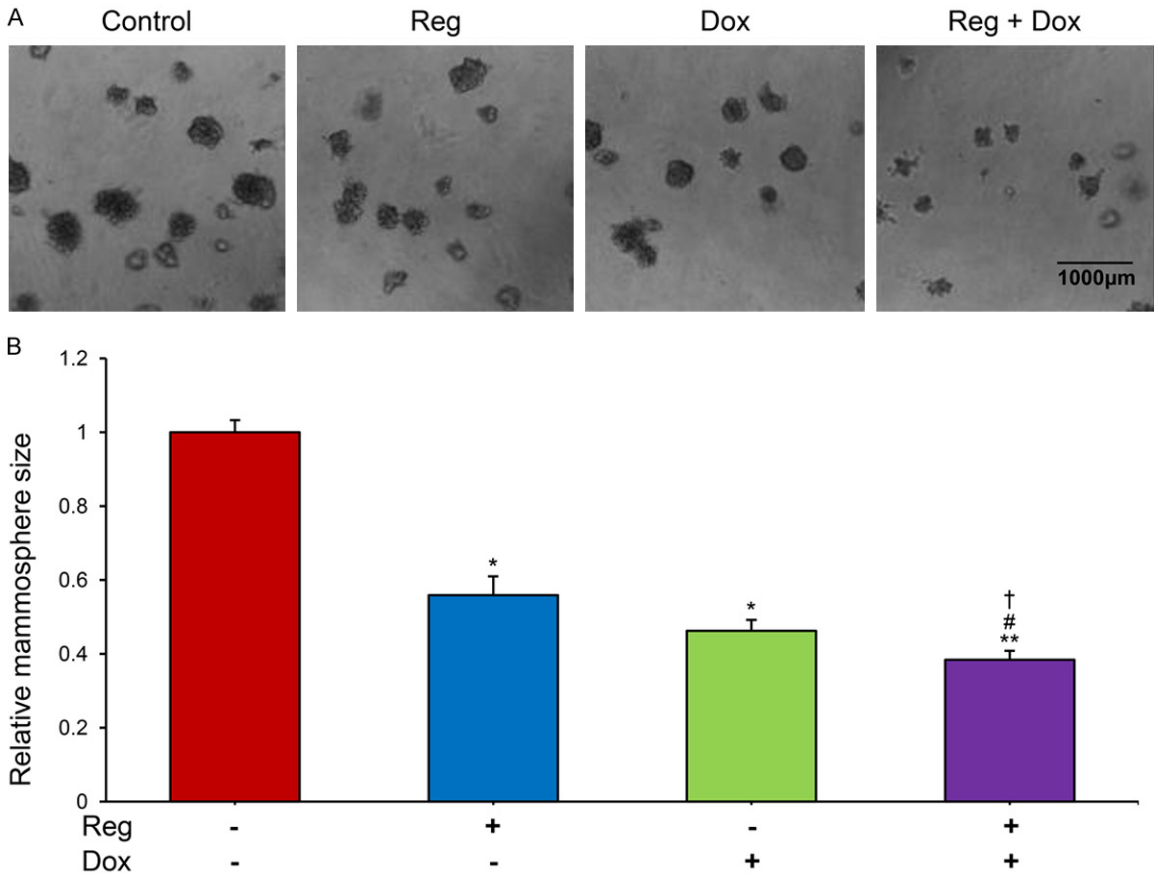

Figure S5. The effect of TOP2A inhibitors combined with regorafenib on cell viability and proliferation. A, B. HepG2-SR and Huh7-SR cells were exposed in the presence or absence of regorafenib (Reg, 7.5 μM) and doxorubicin (Dox, 160 nM), The synergistic reaction of doxorubicin and regorafenib was demonstrated by mammosphere formation (40 ×). $^{*}P$ <0.05 and $^{**}P$ < 0.01 compared with control group, $^{\#}P$ < 0.05, $^{\#\#}P$ < 0.01 compared with regorafenib group. $^{\dagger}P$ < 0.05; $^{\dagger\dagger}P$ < 0.01 compared with siTOP2A treated cells.

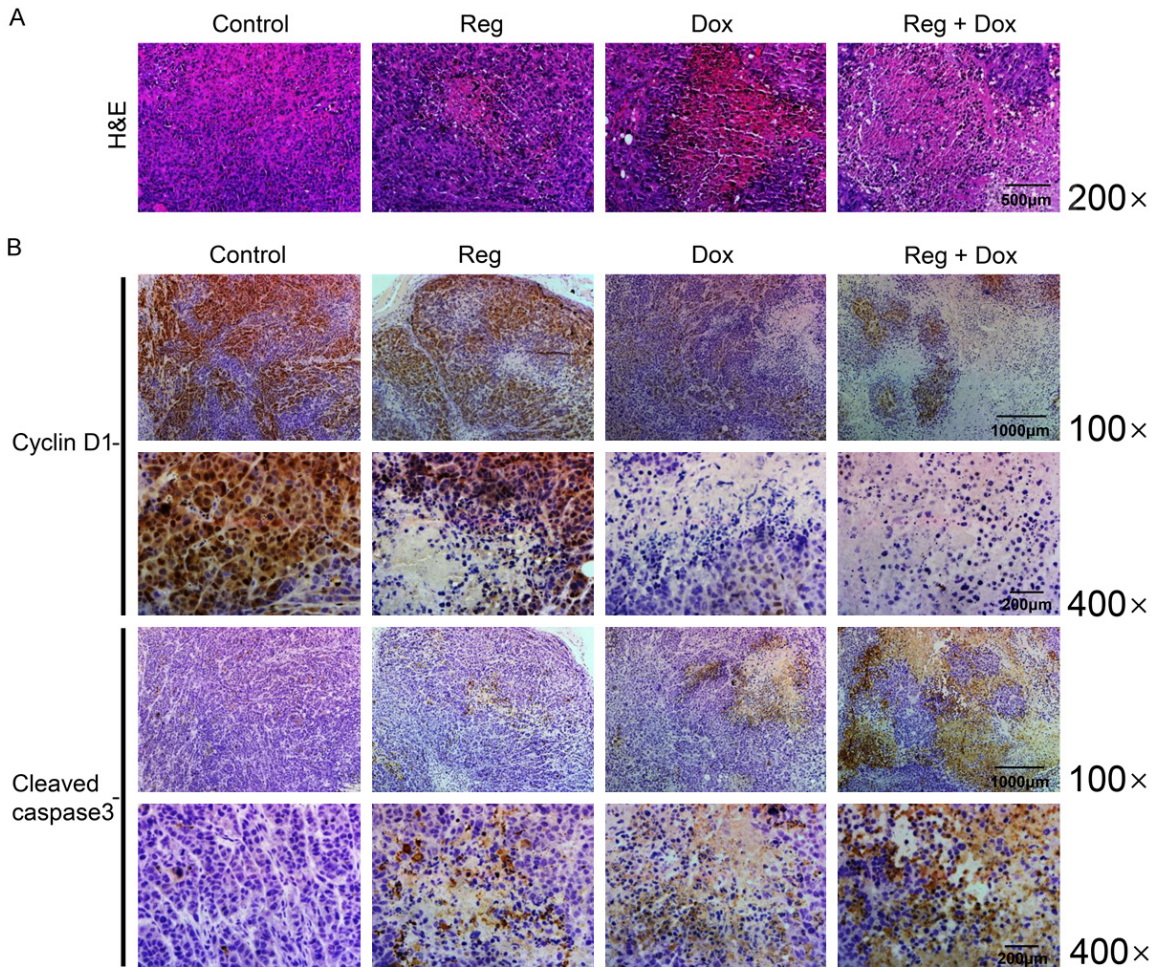

Figure S6. Doxorubicin (Dox) synergizes with Regorafenib (Reg) increases the sensitivity of hepatocellular carcinoma to regorafenib in vitro. (A, B) Hematoxylin and eosin (H&E) staining (magnification, × 200) (A), and immunohistochemistry (IHC) staining (magnification, × 100, × 400) (B) of the tumor.